J. Fluid Mech. (2013), *vol.* 726, *pp.* 517–546.
doi:10.1017/jfm.2013.243

Large-time evolution of statistical moments of wind–wave fields

Sergei Y. Annenkov and Victor I. Shrira†

Department of Mathematics, EPSAM, Keele University, Keele ST5 5BG, UK

(Received 2 October 2012; revised 4 May 2013; accepted 8 May 2013;
first published online 11 June 2013)

We study the long-term evolution of weakly nonlinear random gravity water wave fields developing with and without wind forcing. The focus of the work is on deriving, from first principles, the evolution of the departure of the field statistics from Gaussianity. Higher-order statistical moments of elevation (skewness and kurtosis) are used as a measure of this departure. Non-Gaussianity of a weakly nonlinear random wave field has two components. The first is due to nonlinear wave–wave interactions. We refer to this component as 'dynamic', since it is linked to wave field evolution. The other component is due to bound harmonics. It is non-zero for every wave field with finite amplitude, contributes both to skewness and kurtosis of gravity water waves and can be determined entirely from the instantaneous spectrum of surface elevation. The key result of the work, supported both by direct numerical simulation (DNS) and by the analysis of simulated and experimental (JONSWAP) spectra, is that in generic situations of a broadband random wave field the dynamic contribution to kurtosis is small in absolute value, and negligibly small compared with the bound harmonics component. Therefore, the latter dominates, and both skewness and kurtosis can be obtained directly from the instantaneous wave spectra. Thus, the departure of evolving wave fields from Gaussianity can be obtained from evolving wave spectra, complementing the capability of forecasting spectra and capitalizing on the existing methodology. We find that both skewness and kurtosis are significant for typical oceanic waves; the non-zero positive kurtosis implies a tangible increase of freak wave probability. For random wave fields generated by steady or slowly varying wind and for swell the derived large-time asymptotics of skewness and kurtosis predict power law decay of the moments. The exponents of these laws are determined by the degree of homogeneity of the interaction coefficients. For all self-similar regimes the kurtosis decays twice as fast as the skewness. These formulae complement the known large-time asymptotics for spectral evolution prescribed by the Hasselmann equation. The results are verified by the DNS of random wave fields based on the Zakharov equation. The predicted asymptotic behaviour is shown to be very robust: it holds both for steady and gusty winds.

Key words: surface gravity waves, waves/free-surface flows, wind–wave interactions

1. Introduction

The ultimate aim of all studies of random water wave fields is to predict the probability density function (p.d.f.) of the wave characteristics, primarily wave height,

† Email address for correspondence: v.i.shrira@keele.ac.uk

at any given place and time. A linear wave field is known to obey the stationary Gaussian statistics (e.g. Komen *et al.* 1994), which leads to the Rayleigh distribution for wave heights, under the additional assumption of narrowbandedness of the energy spectrum (Rice 1954; Longuet-Higgins 1957; Goda 2000).

Although linear models do describe major features of wave statistics (Young 1999; Goda 2000), they fail in capturing two principal aspects of reality. First, such models predict no energy exchange between different spectral bands and, correspondingly, no evolution of wave spectra. Such evolution is most prominently manifested by the frequency downshift of the spectral peak. Second, nonlinearity leads to a departure of field statistics from Gaussianity. Although this departure is small for the bulk of the probability distribution, it is not small for the tails of the distribution and, therefore, is crucial for predicting rare anomalously high waves (freak or rogue waves), which is vital for many applications. The slightest difference in the distribution tail shape could result in huge disparities in the probability of freak waves and, correspondingly, significant scatter of 'the highest wave' type estimates required by industry. The observed statistics of such waves deviates significantly from the predictions based upon the Rayleigh distribution (Stansell 2004; Mori & Janssen 2006*a*). Following Tayfun (1980), the effect of nonlinearity through bound harmonics onto wave height distributions started to be taken into account for narrowbanded spectra; skewness was found to be the dominant non-Gaussian effect. In subsequent developments, the approach has been extended to include small but finite spectral width (Fedele & Tayfun 2009). A number of reasonably successful semi-empirical parameterizations of wave height distributions has been developed; in various ways they incorporate a finite spectral width and bound harmonic nonlinearity of the wave field (see references in Fedele 2008; Fedele & Tayfun 2009). However, the available data on statistics of very rare events are naturally quite sparse; correspondingly, because of the lack of solid theoretical foundation the reliability and prognostic value of the parameterizations of the distribution tails remains unknown. In this context, it would be highly desirable to derive wave height distribution from first principles using only transparent and verifiable assumptions. The present work is a contribution towards this goal.

A systematic nonlinear theory of random weakly nonlinear waves starting from first principles is already quite mature, having been successfully developed by efforts of many scientists over the last 50 years. This theory proved to be very good in modelling the observed evolution of wave energy spectra (Hasselmann 1962; Komen *et al.* 1994; Pushkarev, Resio & Zakharov 2003; Janssen 2004). However, the links between the already established laws of wave spectra evolution and those of wave heights distribution are poorly understood. The present work aims at filling this gap.

The established theoretical description of random wind waves is based on the wave (or weak) turbulence paradigm. The wave field is considered as a continuum of resonantly interacting random weakly nonlinear waves. Its natural dynamical description is in terms of nonlinear normal modes in the wavevector space with the bound harmonics eliminated by the canonical transformation (Krasitskii 1994; Janssen 2004). Here, the term 'bound harmonics' refers to all harmonics that are generated by non-resonant nonlinear interactions and do not satisfy the linear dispersion relation, including the higher harmonics of Stokes waves, sum and difference harmonics of the free waves, and combinations of these harmonics with the free waves. In the linear limit, the statistics of a random wave field is Gaussian and stationary. Interactions between the modes due to nonlinearity lead to the wave spectrum evolution and, at the same time, to a departure from Gaussianity. Under the assumption of quasi-Gaussianity it is in principle possible to deduce theoretically the evolution of all

statistical moments and structure functions of a wave field (Nazarenko 2011). However, the realization of this programme is not straightforward and has not been accomplished yet. Over the last 50 years the efforts were concentrated on the evolution of the second moment of a wave field, which represents the energy or wave-action spectrum. In virtually all studies, this evolution was considered to be governed by the kinetic (Hasselmann) equation (KE) (Hasselmann 1962; Zakharov, L'vov & Falkovich 1992). In the KE the nonlinear transfer term is derived via a regular asymptotic procedure based on smallness of nonlinearity and verifiable transparent additional assumptions, which include quasi-Gaussianity (Hasselmann 1962; Zakharov *et al.* 1992; Komen *et al.* 1994; Janssen 2004). A number of parameterizations of wind generation and dissipation terms in the KE is currently in use (Komen *et al.* 1994; Kudryavtsev, Makin & Meirink 2001; Donelan *et al.* 2006; Babanin 2011). The KE underpins operational wave models, which are now an integral part of global weather forecasting. The quality of wave forecasting, in particular that of integral characteristics of wave fields, such as the total energy or position and magnitude of the spectral peak, is quite good (Janssen 2008). Among the key achievements of the theory was the discovery of exact powerlike solutions of the KE (the Kolmogorov–Zakharov spectra) and the realization of their physical significance in terms of direct and inverse cascades of general turbulence (Zakharov *et al.* 1992; Nazarenko 2011). In our context, of special interest is the observation that under steady wind, both the field data (Toba 1972; Young 1999; Badulin *et al.* 2007), and the simulations within the framework of the KE with various parameterizations of wind input and breaking (Badulin *et al.* 2005; Zakharov 2005; Gagnaire-Renoud, Benoit & Badulin 2011) demonstrate that the evolution of wave spectra is self-similar. That is, for sufficiently large times energy E or wave-action n spectra in terms of frequency ω or wavenumber k have a distinct shape characterized by a powerlike spectral slope of the form, e.g. $n \sim \omega^{\lambda}$ with a moving and growing maximum $N_p \sim t^{\alpha}$ at the peak frequency $\omega_p \sim t^{\beta}$, and a sharp front for frequencies below ω_p. The values of λ, α and β are tightly linked and determined by the specific asymptotic regime. A large family of asymptotic regimes exists (Badulin *et al.* 2005; Gagnaire-Renoud *et al.* 2011), notable cases being the regimes linked to constant fluxes of wave energy (Toba 1972), momentum (Hasselmann *et al.* 1976) and wave action (Zakharov & Zaslavsky 1983). It is usually assumed that the majority of cases of wind–wave growth are described by the well-known Toba's '3/2 law' corresponding to the constant flux of energy from wind to waves and $\alpha = 8/3$, $\beta = -1/3$. Another asymptotic regime, associated with a later stage of wave development (Zakharov & Zaslavsky 1983; Gagnaire-Renoud *et al.* 2011), corresponds to constant wave-action flux and $\alpha = 23/11$, $\beta = -3/11$. One of the specific aims of this study is to relate these well-established, both theoretically and experimentally, regimes of wave spectra evolution with their counterparts for the higher moments of wave height distribution.

As was noted above, a linear wave field with Gaussian statistics leads to the Rayleigh distribution for wave heights only under the additional assumption of narrowbandedness of a wave field (Longuet-Higgins 1983). The reason for this counterintuitive constraint is that wave height, obtained by analysing time series of surface elevation, is not a natural quantity in the theoretical context of water wave statistics, being well-defined for a narrowband wave field only. As noted by Goda (2000) '...in fact, there is no absolute method of definition. However, the customary practice ...is to utilize either the zero-upcrossing method or the zero-downcrossing method as the standard techniques for defining waves'. The shortcomings of such definitions are discussed by Janssen (2007), where a much

more theoretically appealing alternative based on the concept of envelope of analytical signal has been put forward. The idea of the analytical signal introduced by Gabor (1946) is widely used in many branches of science. In our context, if we have a time record of surface elevation $\zeta(t)$, one can introduce an analytical signal as $Z(t) = \zeta(t) + \mathrm{i}\xi(t) = \zeta(t) + \mathrm{i}H[\zeta(t)]$, where $H[\zeta(t)]$ is the Hilbert transform of $\zeta(t)$. One can always present $Z(t)$ in polar form, $Z(t) = \rho \mathrm{e}^{\mathrm{i}\varphi}$, where $\rho = \sqrt{\zeta^2 + \xi^2}$, $\varphi = \arctan(\xi/\zeta)$ and $\zeta = \rho\cos\varphi$, $\xi = \rho\sin\varphi$. Thus, ρ is the envelope amplitude and φ is the phase of the signal. It is convenient to define the wave height as 2ρ, which would coincide with the zero-crossing engineering definitions for narrowband spectra. The advantage of this definition is that it applies to arbitrary spectra, including the broadband ones. Then, for linear wave fields the distribution of the wave height defined in this way is the Rayleigh distribution, irrespective of the spectral width. Any other definition of wave height does not have this property for arbitrary spectra. Since there is no established view on how to define maximal wave heights for non-narrow spectra, we will examine the statistics of wave envelope based upon the analytical signal. However, we formulate our results in terms of statistical moments of surface elevation, such as kurtosis and skewness, which are functionals of directly measurable surface elevation and do not depend on the way wave heights are defined. Different applications might rely on different definitions of wave heights; the invariant moments we find are the necessary elements for constructing any p.d.f.

Thus, our main interest in this paper is in the deviations from the Rayleigh distribution of the wave heights due to nonlinearity, manifested in the skewness and kurtosis. While the spectral evolution is reasonably well-understood, effects of nonlinearity on the departure from Gaussianity are less studied. The first major step towards understanding the evolution of wave distributions beyond spectra for generic broadband wave fields was made by Janssen (2003). Staying within the standard kinetic description employed in the derivation of the kinetic (Hasselmann) equation, Janssen (2003, 2009) was able to link the evolution of the third and fourth moments of surface elevation, and the related skewness and kurtosis, to that of the energy spectra. It is beneficial to separate the non-Gaussianity due to resonant interactions of nonlinear normal modes in the canonically transformed space from the effects due to bound harmonics, which are eliminated by the canonical transformation. When the non-Gaussianity is small, the effects due to these contributions just sum up and we gain a better insight by studying them separately. If it is not small, then, strictly speaking, the whole weak turbulence concept underpinning the KE is not applicable.

The first contribution to the non-Gaussianity comes from resonant nonlinear interactions. In the absence of resonant three-wave interactions in a gravity wave field, the quadratic nonlinearity of a wave field is completely excluded by the canonical transformation. Then the wave field in the transformed space becomes Gaussian to this order. Therefore, the lowest-order non-Gaussian effect for the interacting nonlinear normal modes is due to resonant four-wave interactions, manifesting itself in the non-zero kurtosis of the transformed wave field. Following the notation and terminology of Annenkov & Shrira (2009*b*), we will refer to this kurtosis as 'dynamic' and denote it as $C_4^{(d)}$. Generally speaking, the dependence of $C_4^{(d)}$ on wave spectra is non-local in time, i.e. $C_4^{(d)}$ depends on the history of spectral evolution. Assuming that the spectrum is changing slowly on the time scale of the KE solutions, Janssen (2003) expressed $C_4^{(d)}$ explicitly in terms of instantaneous wave-action spectra $n(\boldsymbol{k})$ as an integral over the six-dimensional domain with an oscillating kernel. In the large-time limit, implicitly employed in the standard derivation of the KE, the integral becomes

singular and should be understood as a principal value integral (Janssen 2003, 2004). The further developments (e.g. Mori & Janssen 2006*b*; Onorato *et al.* 2006) were confined to narrowband wave fields, which are of special interest in the context of freak wave formation due to modulational instability. Such narrowband situations, being at the limits, or beyond, of the applicability of weak turbulence theory, are characterized by a significant departure from the Gaussianity. They are short-lived and relatively rare, although they might contribute disproportionately to statistics of freak wave events. A version of this approach is now used for the operational forecasting of freak waves (Janssen & Bidlot 2009).

In this work we are interested not in these rare situations with higher probability of freak wave events, but in the most typical wind–wave fields with broadband spectra. The crucial question is to find the dynamic kurtosis, since its evolution has not been studied before. In this work, we adopt the following strategy. First, we simulate the development of a random wave field under the action of constant wind, for a few different wind speeds, by direct numerical simulation (DNS). Along with the simulations, we find the dynamic kurtosis directly, calculating the correlations between the phases of interacting waves, with ensemble averaging. Then, we make use of the approach developed by Janssen (2003), calculating the dynamic kurtosis as a function of time from the spectra obtained via the DNS. This approach, which involves the evaluation of an integral, derived by Janssen (2003), over all (resonant and non-resonant) interactions, represents a challenging computational problem and has not been used before to estimate the kurtosis for a broadband spectrum. The resulting kurtosis is shown to be in agreement with the kurtosis obtained directly via the DNS. The main conclusion is that the dynamic kurtosis is small in absolute value, of the order $O(10^{-2})$ for a developed wave spectrum generated by a constant wind. A similar result is obtained in the large-time limit of the integral for a model (Joint North Sea Wave Project (JONSWAP)) spectrum, which is chosen as a generic example of mature sea conditions. We also derive the long-term asymptotic of the dynamic kurtosis, based on the self-similar properties of a developed wave field, show that in the self-similar regime of wind–wave field development the kurtosis decays with time as t^s, and find the exponent s of this decay.

These results enable us to conclude that in the generic case of mature wind–wave spectra the dynamic contribution to higher moments is small, so that virtually all non-Gaussianity of a wave field can be described in terms of the canonical transformation. Then, the bound harmonic contribution to the second- and higher-order moments of elevation is straightforward to find, using the integral formulation developed by Janssen (2009). Note that quadratic and cubic nonlinearity affect the wave field p.d.f. in the same order. Janssen (2009) has derived the contributions to the second, third and fourth moments of the envelope elevation, and made a conjecture that the contributions to the second moment cancel out due to symmetry. Here, we prove this conjecture in the general case of a two-dimensional wave field, and use Janssen's formulae to calculate the bound harmonic skewness and kurtosis for the spectra obtained via the DNS. The obtained values of the bound harmonic skewness and kurtosis are typically in the range 0.1–0.5 and thus are at least an order of magnitude larger than the dynamic kurtosis for the developed spectra. Therefore, we confirm that in a generic wind–wave field the bound harmonic contribution to the non-Gaussianity dominates. This fundamental conclusion enables us to find the departure from Gaussianity of an evolving wind–wave field directly in terms of the original physical variables via the formulae for bound harmonic contribution derived by Janssen (2009), provided that the spectrum evolution is known. The bound harmonics kurtosis $C_4^{(b)}$ and skewness $C_3^{(b)}$

can serve as a convenient characteristics of this departure. They can be also used to find all other higher moments, and to reconstruct the p.d.f. of envelope elevation. Since all of the higher moments of wave height distribution obtained in this way are integrals of the spectrum, it is natural to expect that the already established self-similar evolution of the spectra will manifest itself in the corresponding self-similar behaviour of higher moments. In this paper, we first show that under steady wind forcing the skewness and the kurtosis indeed closely follow, although in their own specific way, the spectrum evolution, and derive the self-similar laws for the skewness and kurtosis. For example, for wind waves in the regime of constant wave-action flux the kurtosis asymptotically decays as $t^{-4/11}$ and the skewness decays as $t^{-2/11}$. These analytical results are shown to agree with numerics, both for a wind–wave field generated by constant wind, and for swell. Furthermore, we demonstrate the robustness of these results by extending them numerically to fluctuating winds. Thus, we can speak of the multi-dimensional self-similarity of wave field evolution: each of the higher moments obeys its own law of evolution determined by the specific dynamics of the spectrum.

The paper is organized as follows. In § 2 we present the problem statement and theoretical background. In § 3, the self-similar properties of wind–wave spectra under constant wind are discussed and then used to derive the large-time asymptotics for higher statistical moments of elevation. In § 4, the DNS algorithm, based on the Zakharov equation, is described. In § 5 we discuss the results of numerical simulations. First, we focus on the dynamic non-Gaussianity, using the DNS results to demonstrate that it is indeed small in generic case. Then, the numerical results for bound harmonic skewness and kurtosis are discussed. In particular, the self-similar behaviour, derived analytically in § 3, is demonstrated numerically. Finally, we discuss the results of the simulations with fluctuating or random (gusty) forcing, demonstrating the robustness of the conclusions obtained for the case of the steady forcing. Concluding remarks and a discussion are in § 6. The lengthy formulae for the bound harmonic skewness and kurtosis in terms of the spectrum are given in the Appendix.

2. Theoretical background

2.1. *Evolution of spectra*

The starting point of the analysis is the Zakharov integrodifferential equation for surface gravity waves in deep water, which is derived from the Hamiltonian formulation of primitive water wave equations (Zakharov 1968; Krasitskii 1994). Consider potential gravity waves on the free surface of a homogeneous, incompressible and inviscid fluid of infinite depth, choosing a coordinate system (x, y, z) with the vertical axis z oriented upward, and the origin at the undisturbed water surface. Then the wave motion can be described by two canonical dependent variables $\zeta(x, y, t)$ (the elevation of the surface) and $\psi(x, y, t)$ (the velocity potential at the surface), the total energy of the system being used as the Hamiltonian (Zakharov 1968; Zakharov *et al.* 1992). Introducing Fourier transforms $\hat{\zeta}(\boldsymbol{k}, t)$ and $\hat{\psi}(\boldsymbol{k}, t)$ and Zakharov's canonical complex variables $a(\boldsymbol{k})$,

$$\hat{\zeta}(\boldsymbol{k}) = \left[\frac{q(\boldsymbol{k})}{2\omega(\boldsymbol{k})}\right]^{1/2} \left[a(\boldsymbol{k}) + a^*(-\boldsymbol{k})\right], \quad \hat{\psi}(\boldsymbol{k}) = \left[\frac{\omega(\boldsymbol{k})}{2q(\boldsymbol{k})}\right]^{1/2} \left[a(\boldsymbol{k}) - a^*(-\boldsymbol{k})\right], \tag{2.1}$$

the Hamiltonian evolution equations can be written as

$$\mathrm{i}\frac{\partial a(\boldsymbol{k})}{\partial t} = \frac{\delta H}{\delta a^*(\boldsymbol{k})}, \tag{2.2}$$

where $\boldsymbol{k} = (k_x, k_y)$, the asterisk denotes complex conjugation and $\omega(\boldsymbol{k}) = [gq(\boldsymbol{k})]^{1/2}$ is the linear dispersion relation, $q(\boldsymbol{k}) = |\boldsymbol{k}| = k$ for infinite depth and g is the acceleration due to gravity. The Hamiltonian H is a functional of $a(\boldsymbol{k})$, $a^*(\boldsymbol{k})$, usually written in the form of a series in powers of these variables, utilizing the smallness of nonlinearity.

The Zakharov equation is formulated in terms of new variables $b(\boldsymbol{k})$

$$\mathrm{i}\frac{\partial b_0}{\partial t} = (\omega_0 + \mathrm{i}\gamma_0)\, b_0 + \int T_{0123} b_1^* b_2 b_3 \delta_{0+1-2-3}\, \mathrm{d}\boldsymbol{k}_{123}, \tag{2.3}$$

where $\mathrm{i}\gamma(\boldsymbol{k})$ is the small imaginary correction to frequency describing net forcing, i.e. forcing minus dissipation. Here and below, we use the compact notation that designates the arguments by indices, e.g. $b_0 = b(\boldsymbol{k}_0, t)$, $T_{0123} = T(\boldsymbol{k}_0, \boldsymbol{k}_1, \boldsymbol{k}_2, \boldsymbol{k}_3)$, $\delta_{0+1-2-3} = \delta(\boldsymbol{k}_0 + \boldsymbol{k}_1 - \boldsymbol{k}_2 - \boldsymbol{k}_3)$, $\mathrm{d}\boldsymbol{k}_{123} = \mathrm{d}\boldsymbol{k}_1\, \mathrm{d}\boldsymbol{k}_2\, \mathrm{d}\boldsymbol{k}_3$, $b(\boldsymbol{k}, t)$ is a nonlinear normal variable, linked to $a(\boldsymbol{k}, t)$ through an integral-power series (Krasitskii 1994)

$$\begin{aligned} a_0 = b_0 &+ \int A^{(1)}_{012} b_1 b_2 \delta_{0-1-2}\, \mathrm{d}\boldsymbol{k}_{12} \\ &+ \int A^{(2)}_{012} b_1^* b_2 \delta_{0+1-2}\, \mathrm{d}\boldsymbol{k}_{12} + \int A^{(3)}_{012} b_1^* b_2^* \delta_{0+1+2}\, \mathrm{d}\boldsymbol{k}_{12} + \cdots, \end{aligned} \tag{2.4}$$

which represents a canonical transformation that eliminates non-resonant triplet and quartet interactions. Integration is performed over the entire $\boldsymbol{k}$-plane. Expressions for all kernels in (2.3) and (2.4), as well as all details of the derivation of (2.3), can be found in Krasitskii (1994). The Zakharov equation operates in the canonically transformed space of $b(\boldsymbol{k})$, essentially describing the free-wave part of the wave field. The bound harmonics contribution up to third order in nonlinearity are accounted for by the canonical transformation (2.4).

For the most of practical applications such as wave forecasting, the information on the phases of waves is not available. The phases of the initial state of the wave field are never known, while even small inaccuracies in the initial conditions diverge exponentially with time (Annenkov & Shrira 2001). Therefore, a statistical description is the only meaningful way of describing long-term evolution of nonlinear wind–wave field. The evolution of statistical characteristics of a wave field is usually studied in terms of correlators of $b(\boldsymbol{k}, t)$. The classical derivation (e.g. Zakharov *et al.* 1992) uses (2.3) as the starting point and leads to the equation for the second statistical moment

$$\frac{\partial n_0}{\partial t} = 4\pi \int T^2_{0123} f_{0123} \delta_{0+1-2-3} \delta(\Delta\omega)\, \mathrm{d}\boldsymbol{k}_{123} + S_f, \tag{2.5}$$

where n_0 is the second-order correlator, $\langle b_0^* b_1 \rangle = n_0 \delta_{0-1}$, angular brackets mean ensemble averaging, $f_{0123} = n_2 n_3 (n_0 + n_1) - n_0 n_1 (n_2 + n_3)$, $\Delta\omega = \omega_0 + \omega_1 - \omega_2 - \omega_3$, and S_f is the forcing/dissipation term. The kinetic (Hasselmann) equation (2.5) describes the evolution of the wave spectra in terms of wave action. It assumes a random wave field to be close to Gaussianity and stationarity, which makes (2.5) inapplicable for wave fields far from equilibrium, e.g. subjected to a rapid change of wind (Annenkov & Shrira 2009*a*).

2.2. *Higher statistical moments*

The presence of nonlinear wave interactions leads to evolution of the spectra and to a departure of the field from Gaussianity. The skewness and kurtosis of the field follow from the third and the fourth statistical moments, being a convenient measure of this departure in a generic case.

Let us first consider the non-Gaussianity of the canonically transformed wave field $b(\boldsymbol{k}, t)$, denoting its statistical moments as $m_j, j = 2, 3, 4$. The second moment has the form

$$m_2 = \int \omega_0 b_0 b_0^* \, \mathrm{d}\boldsymbol{k}_0. \tag{2.6}$$

Since in this paper only deep-water gravity waves are considered, the third moment m_3 and, hence, the skewness,

$$C_3^{(d)} = \frac{m_3}{m_2^{3/2}}, \tag{2.7}$$

are identically zero, due to the absence of resonant three-wave interactions. Here and below we use the superscript $^{(d)}$ ('dynamic') to denote the skewness and the kurtosis of the canonically transformed wave field, emphasizing the fact that these quantities can be non-zero only in the presence of nonlinear resonant interactions, within wave triplets and quartets, respectively. The fourth moment m_4 can be calculated from the known wave field $b(\boldsymbol{k}, t)$ as (Janssen 2003)

$$m_4 = \frac{3}{4} \int (\omega_0 \omega_1 \omega_2 \omega_3)^{1/2} \langle b_0^* b_1^* b_2 b_3 \rangle \, \mathrm{d}\boldsymbol{k}_{0123} + \text{c.c.}, \tag{2.8}$$

where c.c. is the complex conjugate, and then the kurtosis $C_4^{(d)}$ is

$$C_4^{(d)} = m_4/m_2^2 - 3. \tag{2.9}$$

Note that $C_4^{(d)}$ cannot be obtained from the simulations of the kinetic equation (2.5). One possible way of calculating it is by DNS, i.e. by integrating the Zakharov equation (2.3) or primitive dynamic equations for the wave field numerically and averaging (2.8) over realizations. This will be done on the basis of the Zakharov equation in the next section.

Another possibility is to use the statistical approach pioneered by Janssen (2003). Here we briefly outline how it can be exploited. Let us first write down the expression for the fourth-order correlator

$$\langle b_0^* b_1^* b_2 b_3 \rangle = n_0 n_1 (\delta_{0-2}\delta_{1-3} + \delta_{0-3}\delta_{1-2}) + J^{(1)}_{0123}\delta_{0+1-2-3}, \tag{2.10}$$

where $J^{(1)}_{0+1-2-3}$ is the fourth-order cumulant. Janssen (2003) made an assumption that the action density $n(\boldsymbol{k}, t)$ evolves on the slow $O(\varepsilon^{-4})$ time scale. Then, employing the standard statistical closure and assuming that $J^{(1)}_{0+1-2-3} = 0$ at the initial moment, Janssen obtained the approximate expression

$$J^{(1)}_{0+1-2-3} = 2T_{0123} R(\Delta\omega, t) f_{0123}, \tag{2.11}$$

where

$$R(\Delta\omega, t) = \frac{\cos(\Delta\omega t) - 1}{\Delta\omega} + \mathrm{i}\frac{\sin(\Delta\omega t)}{\Delta\omega}. \tag{2.12}$$

Using (2.8) and (2.11), the fourth moment can be expressed as

$$m_4 \approx m_4^{(J)} = 3m_2^2 + 3\mathrm{Re} \int T_{0123} (\omega_0 \omega_1 \omega_2 \omega_3)^{1/2} R(\Delta\omega, t) f_{0123} \delta_{0+1-2-3} \, \mathrm{d}\boldsymbol{k}_{0123}, \tag{2.13}$$

where the superscript $^{(J)}$ denotes the approximation suggested by Janssen (2003). Then the kurtosis can be calculated as

$$C_4^{(d)} \approx \frac{3}{m_2^2}\mathrm{Re}\int T_{0123}(\omega_0\omega_1\omega_2\omega_3)^{1/2}R(\Delta\omega,t)f_{0123}\delta_{0+1-2-3}\,\mathrm{d}\boldsymbol{k}_{0123}. \tag{2.14}$$

In the large-time limit adopted in the standard derivation of the kinetic equation, this expression tends to

$$C_4^{(d)} \approx -\frac{3}{m_2^2}\fint_0^\infty T_{0123}(\omega_0\omega_1\omega_2\omega_3)^{1/2}\frac{f_{0123}}{\Delta\omega}\delta_{0+1-2-3}\,\mathrm{d}\boldsymbol{k}_{0123}, \tag{2.15}$$

where Cauchy principal value of the integral is taken. Note that within this approach the kurtosis depends on all interactions except the exactly resonant ones. Approximations (2.14) and (2.15) will be used for the evaluation of the dynamic kurtosis in the next section.

However, even if the wave field in canonical variables $b(\boldsymbol{k},t)$ is Gaussian (for example, if there are no nonlinear interactions close to resonance), in the physical space non-Gaussianity is non-zero for any finite-amplitude wave field, since there is an additional source of non-Gaussianity due to the presence of bound harmonics. This part of the non-Gaussianity is eliminated by the canonical transformation (2.4). For brevity we will refer to it as bound harmonic non-Gaussianity. It is described in the physical space in terms of the surface elevation, and can be calculated from (2.4), provided that the dynamic component is small; otherwise the separation of the two components is not possible.

Let us now assume that the dynamic non-Gaussianity is small and consider the statistical moments of the surface elevation

$$\mu_j = \langle\zeta^j\rangle. \tag{2.16}$$

Janssen (2009) derived expressions for μ_j, $j=2,3,4$, in terms of energy density defined as $E(\boldsymbol{k})=\omega n(\boldsymbol{k})/g$. Note that

$$m_2 = \int \omega_0 b_0 b_0^*\,\mathrm{d}\boldsymbol{k}_0 = g\int E_0\,\mathrm{d}\boldsymbol{k}_0. \tag{2.17}$$

For the second statistical moment in physical space, Janssen (2009) obtained

$$\mu_2 = \langle\zeta^2\rangle = \int E_1\,\mathrm{d}\boldsymbol{k}_1 + \int \left(\mathscr{A}_{1,2}^2 + \mathscr{B}_{1,2}^2 + 2\mathscr{C}_{1,1,2,2}\right)E_1E_2\,\mathrm{d}\boldsymbol{k}_{12}, \tag{2.18}$$

where expressions for coefficients $\mathscr{A}_{1,2}, \mathscr{B}_{1,2}, \mathscr{C}_{1,1,2,2}$ are given in the Appendix. Janssen (2009) showed that in the case of one-dimensional wavevectors the second integral is equal to zero due to symmetry, and made a conjecture that this property also holds in the general two-dimensional geometry. The proof of this conjecture is given in the Appendix. Thus, we can write

$$\mu_2 = \langle\zeta^2\rangle = \int E_1\,\mathrm{d}\boldsymbol{k}_1 = \frac{m_2}{g}. \tag{2.19}$$

The third and fourth moments have the form (Janssen 2009)

$$\mu_3 = \langle\zeta^3\rangle = 3\int \left(\mathscr{A}_{1,2} + \mathscr{B}_{1,2}\right)E_1E_2\,\mathrm{d}\boldsymbol{k}_{12}, \tag{2.20}$$

$$\mu_4 = \langle\zeta^4\rangle = 3\int E_1E_2\,\mathrm{d}\boldsymbol{k}_{12} + 12\int \mathscr{J}_{1,2,3}E_1E_2E_3\,\mathrm{d}\boldsymbol{k}_{123}, \tag{2.21}$$

where

$$\mathscr{J}_{123} = \mathscr{A}_{1,3}\mathscr{A}_{2,3} + \mathscr{B}_{1,3}\mathscr{B}_{2,3} + 2\mathscr{A}_{1,3}\mathscr{B}_{2,3} + \tfrac{1}{2}\mathscr{C}_{1+2-3,1,2,3} + \tfrac{1}{2}\mathscr{D}_{1+2+3,1,2,3}. \quad (2.22)$$

The coefficients are given in the Appendix. Then, we can write out the expressions for the bound harmonic components of skewness and kurtosis as

$$C_3^{(b)} = \frac{\mu_3}{\mu_2^{3/2}}, \quad C_4^{(b)} = \frac{\mu_4}{\mu_2^2} - 3. \quad (2.23)$$

In our context it is important that all coefficients in the expressions for moments, listed in the Appendix, are homogeneous functions of $\boldsymbol{k}$. In particular, $\mathscr{J}_{123}$ is a homogeneous function of degree two, that is

$$\mathscr{J}(\alpha\boldsymbol{k}_1, \alpha\boldsymbol{k}_2, \alpha\boldsymbol{k}_3) = \alpha^2 \mathscr{J}(\boldsymbol{k}_1, \boldsymbol{k}_2, \boldsymbol{k}_3), \quad (2.24)$$

while $\mathscr{A}$ and $\mathscr{B}$ are homogeneous functions of degree one.

3. Self-similarity of spectra and higher statistical moments

The key feature of water wave spectra, observed both experimentally (Hasselmann 1973; Toba 1973) and obtained as numerical solutions of the kinetic equation (2.5) (Badulin *et al.* 2005, 2007; Gagnaire-Renoud *et al.* 2011), is a strong tendency towards self-similar behaviour. There is a rich family of self-similar solutions for different power-law dependencies of wave forcing on fetch or duration of wave growth. In particular, in the duration-limited (spatially homogeneous) case, the wave-action spectrum $n(k, t)$, $k = |\boldsymbol{k}|$, tends to the form (Badulin *et al.* 2005; Gagnaire-Renoud *et al.* 2011)

$$n(k, t) = a_B t^{\alpha} \mathscr{U}\left(b_B k t^{\beta}\right), \quad (3.1)$$

where $\mathscr{U}$ is a self-similar function, $\alpha = (19\beta - 2)/4$, a_B and b_B are constant for a specific asymptotic regime. Under wind forcing, the magnitude of the self-similar solution (3.1) grows with time ($\alpha > 0$), while the characteristic frequency (or wavenumber) decreases ($\beta > 0$). Total wave action N_{tot}, energy E_{tot} and momentum M_{tot} grow as

$$N_{tot} \sim t^r, \quad r = \alpha - 2\beta, \quad (3.2a)$$

$$E_{tot} \sim t^p, \quad p = \alpha - 5\beta/2, \quad (3.2b)$$

$$M_{tot} \sim t^m, \quad m = \alpha - 3\beta. \quad (3.2c)$$

Our aim is to derive the asymptotic properties of moments μ_2, μ_3, μ_4 and the 'dynamic' moment m_4 capitalizing on the above asymptotics for N_{tot}, E_{tot} and M_{tot}.

Let us first assume that wave field $b(\boldsymbol{k}, t)$ is free, i.e. $C_4^{(d)}$ is negligible. Then, substituting (3.1) into (2.19) and employing a change of variable $\xi = b_B k t^{\beta}$, $\mathrm{d}\boldsymbol{k} = k\,\mathrm{d}k\,\mathrm{d}\theta$, we obtain

$$\mu_2 = \frac{a_B}{b_B^2} t^{\alpha - 2\beta} \int \omega_1 \mathscr{U}_1 \xi_1 \,\mathrm{d}\xi_1 \,\mathrm{d}\theta_1, \quad (3.3)$$

where $\mathscr{U}_1 = \mathscr{U}(\xi_1)$. Using the long-term asymptotics of the frequency downshift $\omega \sim t^{-\beta/2}$, which follows from (3.1), we obtain

$$\mu_2 = c_2 t^{p_2}, \quad (3.4)$$

where c_2 is a constant and $p_2 = \alpha - 5\beta/2$. The value of p_2 corresponds to the exponent for energy growth in (3.2*b*).

Similarly, substituting (3.1) into (2.20), we get

$$\mu_3 = 3\frac{a_B^2}{b_B^4} t^{2\alpha-4\beta} \int \left[\mathscr{A}(\boldsymbol{k}_1, \boldsymbol{k}_2) + \mathscr{B}(\boldsymbol{k}_1, \boldsymbol{k}_2)\right] \omega_1\omega_2\mathscr{U}_1\mathscr{U}_2\xi_1\xi_2 \,\mathrm{d}\xi_{12}\,\mathrm{d}\theta_{12}. \tag{3.5}$$

Then, using the fact that both $\mathscr{A}$ and $\mathscr{B}$ are homogeneous functions of degree one,

$$\mu_3 = c_3 t^{p_3}, \tag{3.6}$$

where $p_3 = 2(\alpha - 3\beta)$. For the fourth moment,

$$\begin{aligned}\mu_4 = {} & 3\frac{a_B^2}{b_B^4} t^{2\alpha-4\beta} \int \omega_1\omega_2\mathscr{U}_1\mathscr{U}_2\xi_1\xi_2 \,\mathrm{d}\xi_{12}\,\mathrm{d}\theta_{12} \\ & + \frac{a_B^3}{b_B^6} t^{3\alpha-6\beta} \int \mathscr{J}(\boldsymbol{k}_1, \boldsymbol{k}_2, \boldsymbol{k}_3)\omega_1\omega_2\omega_3\mathscr{U}_1\mathscr{U}_2\mathscr{U}_3\xi_1\xi_2\xi_3 \,\mathrm{d}\xi_{123}\,\mathrm{d}\theta_{123},\end{aligned} \tag{3.7}$$

which, using the second-degree homogeneity of $\mathscr{J}$, yields

$$\mu_4 = c_4 t^{2p_2} + d_4 t^{p_4}, \tag{3.8}$$

where $p_4 = 3\alpha - 19\beta/2$. All of the coefficients c_j and d_j are constants.

Substituting the expressions for μ_j, $j = 2, 3, 4$, into (2.23), we obtain the following large-time asymptotics for bound harmonics skewness and kurtosis:

$$C_3^{(b)} \sim t^{q/2}, \quad C_4^{(b)} \sim t^q. \tag{3.9}$$

where $q = \alpha - 9\beta/2$.

Let us now consider estimate (2.13) for the dynamic fourth moment m_4. Again substituting the self-similar form (3.1) into (2.13), we obtain

$$\begin{aligned}m_4^{(J)} = {} & 3m_2^2 + 3\frac{a_B^3}{b_B^6} t^{3\alpha-6\beta} \\ & \times \mathrm{Re} \int T_{0,1,2,0+1-2}(\omega_0\omega_1\omega_2\omega_{0+1-2})^{1/2} R(\Delta\omega, t)\mathscr{F}_{012}\xi_0\xi_1\xi_2 \,\mathrm{d}\xi_{012}\,\mathrm{d}\theta_{012},\end{aligned} \tag{3.10}$$

where

$$\mathscr{F}_{012} = \mathscr{U}_2\mathscr{U}_{0+1-2}(\mathscr{U}_0 + \mathscr{U}_1) - \mathscr{U}_0\mathscr{U}_1(\mathscr{U}_2 + \mathscr{U}_{0+1-2}). \tag{3.11}$$

The factor $\mathrm{Re}[R(\Delta\omega, t)]$ for large time tends to the generalized function $P/\Delta\omega$, where P means the Cauchy principal value (Janssen 2003). The four-wave interaction coefficient T is a homogeneous function of degree three. Taking this into account, and again using the long-term asymptotics of the frequency downshift, we obtain

$$m_4 = 3c_2^2 t^{2p_2} + \tilde{c}_4 t^{p_4}, \tag{3.12}$$

with some constant coefficient $\tilde{c}_4$. Then, the large-time asymptotics for the dynamic kurtosis is

$$C_4^{(d)} \sim t^q, \tag{3.13}$$

and thus the dynamic and the bound-harmonic kurtosis decay at the same rate, for all asymptotic regimes with $q < 0$.

In the generic self-similar form (3.1), it is illuminating to focus upon specific values of α and β corresponding to distinguished asymptotic regimes characterized by constant fluxes of energy, wave action or wave momentum. For these regimes one of

Regime	α	β	p_2	p_3	p_4	q
Constant momentum flux	25/7	6/7	10/7	2	18/7	−2/7
Constant energy flux	8/3	2/3	1	4/3	5/3	−1/3
Constant action flux	23/11	6/11	8/11	10/11	12/11	−4/11
Swell	4/11	2/11	−1/11	−4/11	−7/11	−5/11

TABLE 1. Self-similarity parameters (α, β) and exponents for higher moments for distinguished asymptotic regimes corresponding to constant fluxes and for swell.

the exponents in (3.2*a*) is equal to unity. These asymptotic regimes were known for a long time in terms of parametric laws linking significant wave height and frequency of the wave peak. For the original descriptions of the regimes see Toba (1972) for the regime of constant energy flux, Hasselmann *et al.* (1976) for constant momentum flux, and Zakharov & Zaslavsky (1983) for the regime of constant action flux to waves. The parameters of these distinguished cases are listed in table 1, with the corresponding exponents for moments. Similar results can be obtained for the corresponding regimes in the case of fetch-limited growth (e.g. Gagnaire-Renoud *et al.* 2011).

The above results for the bound harmonics moments are valid only if the dynamic contribution to non-Gaussianity is small, i.e. $C_4^{(d)} \ll 1$. We have shown that in the self-similar regime of spectrum evolution $C_4^{(d)}$ always decays, but so far have not discussed the sign and absolute value of $C_4^{(d)}$. In § 5, these values will be obtained numerically.

4. Numerical algorithm

In this paper, we are studying the evolution of higher statistical moments of a wave field, which cannot be obtained within the standard statistical approach based on the kinetic equation. Hence, we need to reproduce the evolution of a wave field with a DNS algorithm, obtaining, under some standard forcing and dissipation, wave spectra and other characteristics. At present, the algorithm described in this section is the only existing DNS algorithm for water waves capable to trace the evolution of a random wave field generated by realistic wind for sufficiently long time, exceeding 10^4 characteristic wave periods. Previously, it has been successfully used to verify by DNS the self-similarity properties of the kinetic equation (Annenkov & Shrira 2006*b*), and to model the adjustment of a wave field to instantly changing (Annenkov & Shrira 2009*a*) or rapidly fluctuating (Annenkov & Shrira 2011) forcing. Here we will use it for the simulation of higher statistical moments of a wave field. In this section, we will describe the concept and implementation of the algorithm.

The algorithm is based on the efficient numerical scheme built for the integration of the Zakharov equation (2.3) and used for the study of wave dynamics (Annenkov & Shrira 2001). However, the application of the dynamical algorithm for the study of wave statistics has to overcome one substantial difficulty. For numerics, a continuous wave field needs to be discretized, i.e. the complex amplitude $a(\boldsymbol{k}, t)$ or $b(\boldsymbol{k}, t)$ must be replaced by a set of N discrete variables

$$b(\boldsymbol{k}, t) = \sum_{j=1}^{N} b_j(\boldsymbol{k}_j, t). \tag{4.1}$$

Most numerical models of the evolution of weakly nonlinear waves employ a fast Fourier transform on each step, which requires a regular grid. The Zakharov equation allows the use of an arbitrary grid (Annenkov & Shrira 2001). However, for any grid the resulting discrete wave system will have properties differing from those of a continuous wave field. For example, the use of regular grids for the numerical simulation of wave turbulence leads to 'frozen turbulence' effects, due to the insufficient number of resonant and approximately resonant interactions (Pushkarev & Zakharov 2000). A simple estimate of Lvov, Nazarenko & Pokorni (2006) shows that for the resonant interactions to be fully efficient, one must have a computational box far beyond the present computational capacity. Meanwhile, in order to model a continuous wave field correctly, every degree of freedom of a discretized wave field is expected to interact with every other degree of freedom. This means that we need, instead of a straightforward discretization, to work out the concept of coarse-graining of the continuous wave field, which would retain its fundamental properties of nonlinear interactions.

To that end, we build in Fourier space a grid consisting of $\sim 5 \times 10^3$ wavepackets, coupled through exact and approximate resonant interactions. A wavepacket, centred at $\boldsymbol{k}_0$, is characterized by one amplitude and one phase, but has finite bandwidth in Fourier space, and is allowed to enter into nonlinear interactions with other wavepackets, provided that the wavevector mismatch

$$\Delta \boldsymbol{k} = \boldsymbol{k}_0 + \boldsymbol{k}_1 - \boldsymbol{k}_2 - \boldsymbol{k}_3 \tag{4.2}$$

does not exceed a certain threshold (the coarse-graining parameter). Thus, the standard resonance condition $\boldsymbol{k}_0 + \boldsymbol{k}_1 - \boldsymbol{k}_2 - \boldsymbol{k}_3 = 0$ is relaxed. It has been verified that we need to consider only resonant and approximately resonant interactions, prescribing a similar condition on the frequency mismatch $\Delta\omega$, where

$$\Delta\omega = \omega_0 + \omega_1 - \omega_2 - \omega_3. \tag{4.3}$$

In more practical terms, the following condition is formulated: a quartet of grid points is assumed to be in approximate resonance if its wavevector and frequency mismatch satisfies

$$\Delta\omega/\omega_{min} < \lambda_\omega, \quad |\Delta \boldsymbol{k}|/k_{min} < \lambda_k \bar{\omega}/\omega_{min}, \tag{4.4}$$

where $\Delta\omega$ and $|\Delta \boldsymbol{k}|$ are the frequency and wavevector mismatch in the quartet, ω_{min} and k_{min} are the minimum values of frequency and wavenumber in the quartet, $\bar{\omega}$ is the mean frequency and λ_ω and λ_k are the detuning parameters, chosen to ensure that the total number of resonances is $O(N^2)$, where N is the number of grid points. The resulting system of N discrete equations can be integrated in time by a standard Runge–Kutta scheme.

Previously, the algorithm was tested to provide good agreement with the kinetic equation where the latter is applicable (Annenkov & Shrira 2006*a*,*b*), and then used for the study of the wave field 'fast' evolution, when the standard statistical theory cannot be applied (Annenkov & Shrira 2009*a*). For this study, the grid of N wavepackets is logarithmic in the wavenumber k (161 points within a span $0.13 < k < 2.12\ \mathrm{m}^{-1}$) and regular in the angle θ (31 point within $-\pi/3 \leqslant \theta \leqslant \pi/3$, $N = 4991$ and $\lambda_\omega = \lambda_k = 0.01$. The total number of resonant and near-resonant interactions is approximately 5.4×10^7. Results were verified to be non-dependent on specific values in a wide range of λ_ω, λ_k. Initial phases of waves are chosen randomly, and averaging over 30 realizations is performed. A typical DNS computation of one realization took a few hours of parallel computation on 64 Opteron CPU cores.

An important part of a numerical model of wind–wave evolution is the parametrization of wind input and dissipation. Here, we make no attempt to model these terms in all their complexity. Wind input is introduced in a simple form prescribed by the empirical formula by Hsiao & Shemdin (1983), with an additional simplifying assumption that all forcing is confined to the relatively narrow range $1.0 < k < 1.29$ m^{-1}. This allows us to model the long-term evolution of mature waves, where wind input in the part of the spectrum that is close to the peak is approximately balanced by dissipation, without having a long wavenumber spectrum, which would be difficult to obtain with DNS. Dissipation is applied to $k > 1.62$ m^{-1}. While discussing the numerical results, we will quantify the wind input by the wind speed value used in the formula by Hsiao & Shemdin (1983). Simulations without the simplifying assumption of spectrally confined forcing were found to produce similar outcome; since such simulations are considerably more expensive computationally they were not used for ensemble averaging.

The statistical moments m_2, m_3, m_4 are computed from wave-action spectra $n(\boldsymbol{k})$ by numerical evaluation of the integrals in (2.19)–(2.21). The evaluation of the triple integral in (2.21) requires substantial computational resources, and it is computed using the grid with angle resolution reduced by a factor of two. Computations of moments are performed for $k < 2.5k_p$, where k_p in the wavenumber of the spectral peak, specified as the local maximum of $n(\boldsymbol{k})$. Employing DNS, we were also able to trace the evolution of the dynamic part of kurtosis $C_4^{(d)}$, using formulae (2.8)–(2.9) and averaging over realizations.

5. Evolution of wind-generated waves

5.1. *Constant forcing*

We start this section with presenting the results of the DNS of random wind–wave fields generated by a steady wind. In the simulations, a broadbanded wave field is generated by constant wind, starting with a low-intensity white noise, and then its evolution is traced up to a few thousand characteristic wave periods τ, until the wave field is well into the self-similar regime. Here and below we use the period of the wave with $\omega = 2.14$ s^{-1}, approximately corresponding to the peak frequency of the developed spectra in all simulations, as a characteristic wave period. A few values of wind speed in the range 6–20 m s^{-1} are used. Wind forcing, specified by the parametrization of Hsiao & Shemdin (1983), is applied to the high-frequency part of the spectrum only ($\omega > 3.13$ s^{-1}), so that the most energetic part of a developed wave field evolves entirely due to nonlinear interactions.

An example of evolution of the wave-action wavenumber spectrum $n(\boldsymbol{k})$ is shown in figure 1, for wind speed $U = 12$ m s^{-1}. Steepness ε and mean wave height H_{rms} are defined as

$$H_{rms} = \int 2E(\boldsymbol{k})\,\mathrm{d}\boldsymbol{k}, \quad E(\boldsymbol{k}) = \frac{\omega n(\boldsymbol{k})}{g}, \quad \varepsilon = \frac{1}{2}H_{rms}k_p, \tag{5.1}$$

where k_p is the wavenumber of the spectral peak, specified as the local maximum of $n(\boldsymbol{k})$. Evolution of ε and H_{rms} for various values of constant wind speed in the range 6–20 m s^{-1} is shown in figure 2(*a*,*b*).

5.2. *Dynamic non-Gaussianity*

In this paper, we are interested in the evolution of higher statistical moments of the wave field, primarily skewness and kurtosis. The key task is to estimate the value of

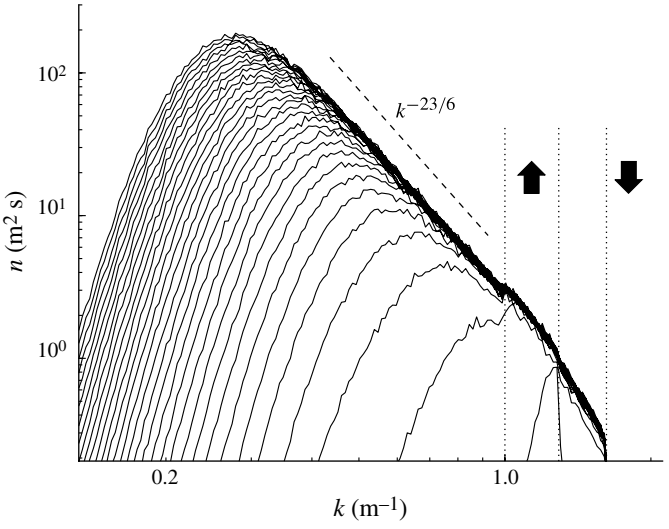

FIGURE 1. An example of evolution of wave-action wavenumber spectrum $n(k)$ under constant wind speed $U = 12$ m s^{-1}. Curves are drawn in steps of approximately 400 characteristic wave periods, spectral regions of forcing and dissipation are shown by up and down arrows, respectively.

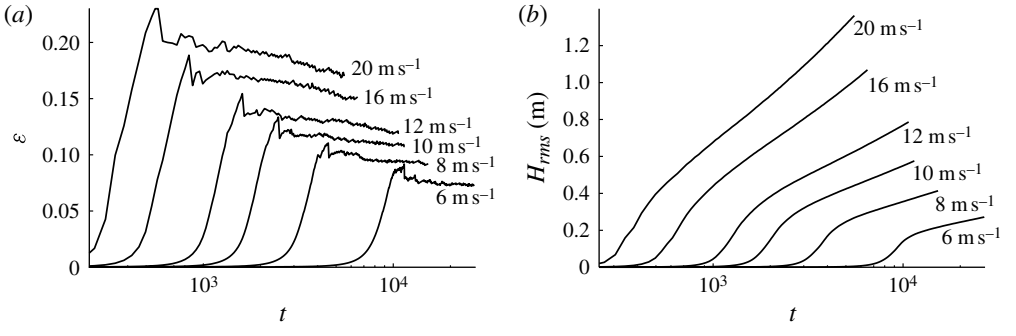

FIGURE 2. Evolution in time of (*a*) wave steepness and (*b*) wave height H_{rms} for waves generated by constant wind in the range 6–20 m s^{-1}. Here and in subsequent figures, time is measured in characteristic wave periods $\tau = 2\pi/2.14$ s, approximately corresponding to the dominant wave period of developed spectra.

the dynamic kurtosis $C_4^{(d)}$. Previously it was found that the kurtosis can be $O(1)$ large for a one-dimensional narrowband wave field (e.g. Janssen 2003), but no information on its value is available for a generic two-dimensional broadband wave field generated by a realistic wind.

We use two different approaches. First, we make use of the information on the phases of interacting waves, available in each DNS realization, to calculate the real part of the fourth-order cumulant, and then the kurtosis. This approach uses the same grid of harmonics and the same set of approximately resonant interactions as the DNS, so that only the interactions that contribute to the spectral evolution (that is,

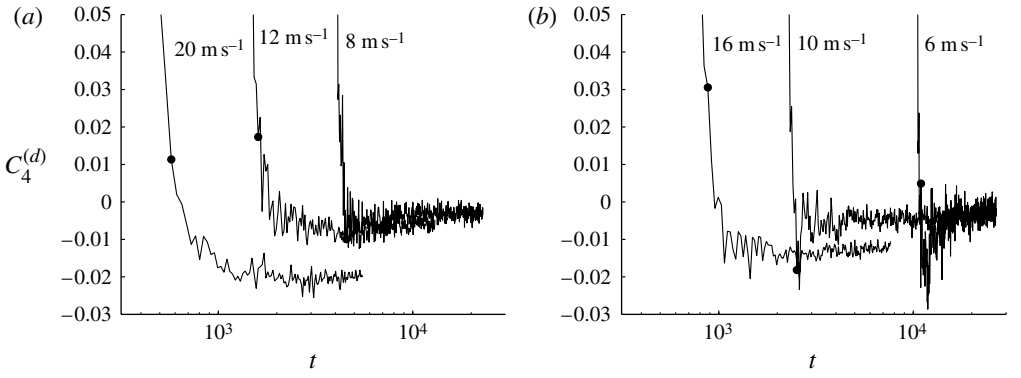

FIGURE 3. Evolution of dynamic kurtosis $C_4^{(d)}$ for waves generated by constant wind with speed (*a*) 8, 12 and 20 m s^{-1} and (*b*) 6, 10 and 16 m s^{-1}, calculated using (2.8)–(2.9). Integration in (2.8) is performed over the resonant and approximately resonant nonlinear interactions taken into account in the DNS of the spectral evolution, with averaging over 30 realizations. Dots show the time when the maximum of steepness is reached (cf. figure 2*a*). The part of the spectrum under the direct wind forcing ($\omega > 3.13$ s^{-1}) is excluded from the computations. The initial part of the evolution is not shown. Time is measured in characteristic wave periods, as in figure 2.

near-resonant interactions satisfying (4.4)) are accounted for in the calculation of the dynamic kurtosis. In figure 3, we show the evolution of $C_4^{(d)}$, calculated from the DNS solution using (2.8)–(2.9). The part of the spectrum which is under the direct wind forcing ($\omega > 3.13$ s^{-1}) is excluded from the computation; this has negligible effect on kurtosis of a well-developed spectrum, when the most energetic waves are far from the forcing domain.

The results show that $C_4^{(d)}$ can be large during the initial part of the wave field evolution, corresponding to the linear stage of wave spectrum development. Transition of a wave field to nonlinear regime of evolution occurs near the maximum of steepness (cf. figure 2*a*); this moment is marked with dots in figure 3. Later, in the nonlinear stage, dynamic kurtosis tends to a small value, not exceeding 0.02 in absolute value for the considered range of wind speeds. For large time this value is negative and nearly constant, approximately scaled as square of wind speed.

It is important to note that the DNS only takes into account nearly resonant interactions. While it has been verified that the interactions further away from resonance do not contribute to the spectral evolution in any noticeable way, it cannot be guaranteed that they do not contribute to the dynamic kurtosis. Although the DNS with all non-resonant interactions included would have been impossible, it is technically possible to include all interactions into the kurtosis calculation once the amplitudes and phases of all harmonics are found via the DNS. However, the approach that accounts for correlations between all combinations of harmonics, but is still based on the DNS of the evolution with the account for near-resonant interactions only, would be inconsistent, since the phases of harmonics that are not linked by nonlinear interactions should be formally considered as uncorrelated. For this reason, we consider the kurtosis obtained by DNS as an estimate.

To provide an alternative estimate, we perform the calculation of the dynamic kurtosis using only the information about the wave spectra, obtained either by DNS

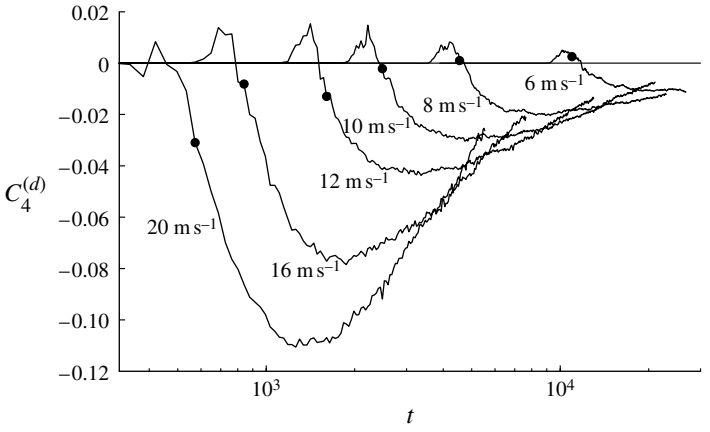

FIGURE 4. Evolution of dynamic kurtosis $C_4^{(d)}$ for waves generated by constant wind in the range 6–20 m s^{-1} , calculated using (2.14) and the spectra obtained by DNS. Grid used in computations is the same as that used for the DNS. Dots show the time when the maximum of steepness is reached (cf. figure 2*a*). The part of the spectrum under the direct wind forcing ($\omega > 3.13$ s^{-1}) is excluded from the computations. The initial part of the evolution ($t < 300$) is not shown. Time is measured in characteristic wave periods, as in figure 2.

or taken from observations. This approach is based on the approximate formulae (2.13) and (2.14), derived by Janssen (2003) under the assumption that the spectrum is evolving slowly. Within this approach, the dynamic kurtosis is determined by the instantaneous spectrum and depends on all nonlinear interactions, including approximately resonant and non-resonant interactions. In figure 4, we plot the dynamic kurtosis calculated from the DNS spectra, using the DNS numerical grid, but, unlike in the DNS case, accounting for all nonlinear interactions (the total number is 1.3×10^{10}). For this purpose, a special numerical approach with the parallel processing of interactions was worked out. To avoid the loss of accuracy due to small denominators at the exact resonance, interactions with $\Delta\omega/\omega_{min} \leqslant 10^{-4}$ were excluded. The results were verified to be not sensitive to the chosen value of the cutoff in $\Delta\omega/\omega_{min}$. Again, we excluded from the computation the part of the spectrum under the direct forcing; this has been verified to have negligible effect on the value of kurtosis in the nonlinear regime of spectrum development. For all values of wind speed, $C_4^{(d)}$ is again negative. For the strongest wind, the value of $C_4^{(d)}$ for a short time can exceed 0.1 in absolute value during the initial fast downshift of the spectral peak (note that (2.14), strictly speaking, is not applicable at the fast stage of the spectral development). During the subsequent evolution, $C_4^{(d)}$ approaches zero, being of the order $O(10^{-2})$ for the times exceeding several times the characteristic time scale of establishing of the nonlinear regime.

Using the same numerical method, we have also calculated the dynamic kurtosis of several empirical (JONSWAP) parameterizations of spectra (e.g. Young 1999)

$$E(\boldsymbol{k}) = \frac{\alpha}{2k^3} \exp\left[-\frac{5}{4}\left(k/k_p\right)^{-2}\right] \gamma^{\exp[-(\sqrt{k/k_p}-1)^2/(2\sigma_A^2)]} D(\theta), \tag{5.2}$$

γ	ε	$C_4^{(d)}$
1.0	0.1	0.017
3.3	0.125	−0.001
10	0.168	−0.070

TABLE 2. Steepness ε and dynamic kurtosis $C_4^{(d)}$ for the JONSWAP spectrum with $\alpha = 0.0258$, $k_p = 1$, $N = 10$ and different values of the peakedness parameter γ, calculated using (2.15).

where $E(\boldsymbol{k}) = \omega(\boldsymbol{k})n(\boldsymbol{k})/g$, $\boldsymbol{k} = k(\cos\theta, \sin\theta)$,

$$D(\theta) = \frac{1}{k\sqrt{\pi}} \frac{\Gamma(N/2+1)}{\Gamma(N/2+1/2)} \cos^N\theta, \tag{5.3}$$

Γ is the gamma function, $\sigma_A = 0.07$ for $k \leqslant k_p$ and 0.09 for $k > k_p$. We have chosen $N = 10$, corresponding to a spectrum with wide angular spreading, $k_p = 1$ and $\alpha = 0.0258$, so that the steepness $\varepsilon = 0.1$ for $\gamma = 1$. An extended numerical grid with 200 logarithmically spaced values of ω in the range $0.5\omega_p \leqslant \omega \leqslant 3.0\omega_p$, where $\omega_p = 3.13\ \mathrm{s}^{-1}$, and 75 values of θ in the range $-\pi/2 < \theta < \pi/2$ were used, corresponding to the total number of interactions exceeding 10^{12}. The computation time for one spectrum was about 1 week on 64 Opteron CPU cores. The dynamic kurtosis was calculated in the large-time limit, using the principal value integral (2.15). Again, we have excluded the nearly exactly resonant interactions with $\Delta\omega/\omega_{min} \leqslant 10^{-4}$. In table 2 we show the values of the dynamic kurtosis $C_4^{(d)}$ for three characteristic values of the peakedness parameter: $\gamma = 1$, corresponding to a mature sea state, $\gamma = 3.3$, typical of relatively young wind–wave fields (JONSWAP experiment average), and $\gamma = 10$, corresponding to a very young wave field. Except for the latter case, the kurtosis is found to be of the order of $O(10^{-2})$.

These results, obtained by different methods, lead to the conclusion that at the nonlinear stage of wind–wave field evolution the dynamic kurtosis is typically small ($C_4^{(d)} \ll 1$) and is decreasing with time. In this work, we have made no attempt to check numerically the theoretical rate of this decrease (3.13). Note that the DNS are not exactly self-similar, due to the fact that the forcing and dissipation are set for fixed wavenumber bands. In order to study the self-similar evolution of the dynamic kurtosis, one has to consider the most energetic waves only, limiting the computations to wavenumbers $k \leqslant Mk_p$, where k_p is the wavenumber of the spectral peak, and M cannot be large, since the DNS spectra are rather short in Fourier space, due to the unavoidable computational limitations of the DNS approach. This could lead to the dynamic kurtosis being underestimated, so the self-similar properties of the dynamic kurtosis were not studied in this paper. The main conclusion, however, is the smallness of the dynamic kurtosis in typical conditions or for large time. This conclusion justifies *a posteriori* the derivation of the bound harmonics skewness and kurtosis in § 2.2.

5.3. *Non-Gaussianity due to bound harmonics*

Now we can proceed to the numerical calculation of bound harmonics skewness $C_3^{(b)}$ and kurtosis $C_4^{(b)}$. Since we are interested in the properties of the self-similar evolution of $C_3^{(b)}$ and $C_4^{(b)}$, the computation is limited to wavenumbers $k \leqslant 2.5k_p$, where k_p is the wavenumber of the spectral peak.

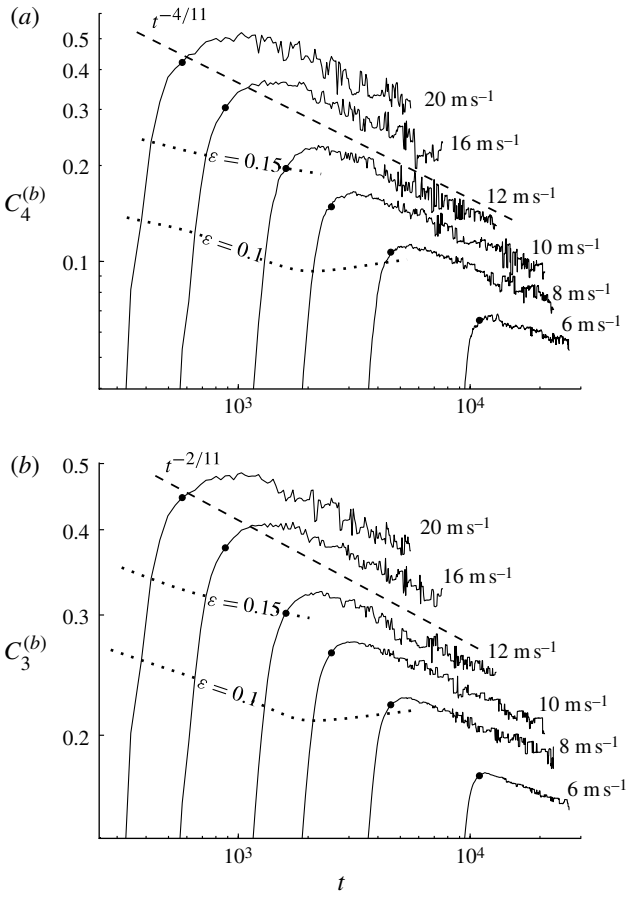

FIGURE 5. Evolution of (*a*) bound harmonic kurtosis $C_4^{(b)}$ and (*b*) skewness $C_3^{(b)}$ for a wave field generated by constant wind of different speeds, in the range 6–20 m s^{-1}, calculated using (2.23). Computation is limited to $k \leqslant 2.5k_p$, where k_p is the wavenumber of the spectral peak. The initial part of the evolution is not shown. Dashed lines show theoretical asymptotics for large time. Dotted curves correspond to values of wave steepness reached during the wave field development. Large dots show the time when the maximum of steepness is reached (cf. figure 2*a*). Time is measured in characteristic wave periods, as in figure 2.

Evolution in time of skewness and kurtosis under constant wind in the range 6–20 m s^{-1}, obtained using (2.19)–(2.23), is shown in figure 5. Under steady wind, the evolution of the developed spectrum is slow and is described by large-time asymptotics of the kinetic equation, corresponding to the constant wave-action flux regime in table 1. Kurtosis $C_4^{(b)}$ is much larger in absolute value than the dynamic kurtosis and positive, slowly decreasing with the powerlike increase of the total energy. The rate of decrease is close to the theoretical rate $\sim t^{-4/11}$. Skewness $C_3 = C_3^{(b)}$ does not have a dynamic part, and its evolution for large time also follows the theoretical rate $\sim t^{-2/11}$.

All curves in figure 5 have universal behaviour, which becomes evident when both $C_3^{(b)}$ and $C_4^{(b)}$ are rescaled by $\sqrt{U}$ and U respectively. This is shown in figure 6, which demonstrates that the rescaled skewness and kurtosis collapse onto a single universal curve with powerlike dependence on time, not depending on the value of forcing.

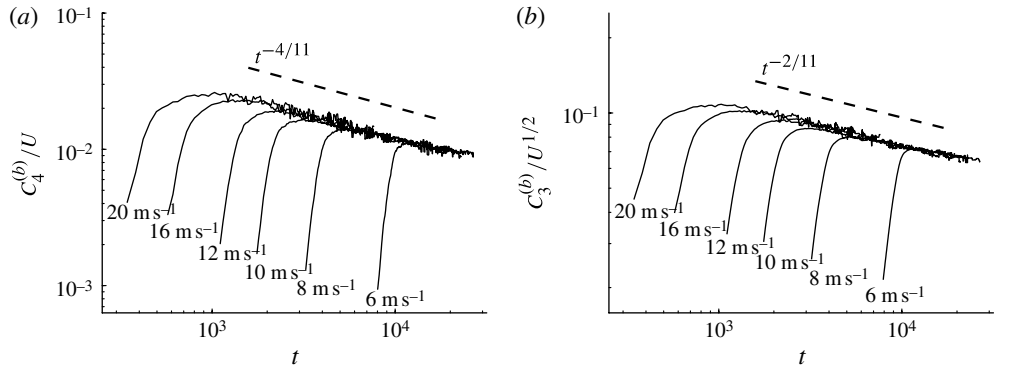

FIGURE 6. Evolution of (*a*) bound harmonics kurtosis $C_4^{(b)}$ and (*b*) skewness $C_3^{(b)}$, shown in figure 5, normalized by wind speed U and by $U^{1/2}$, respectively.

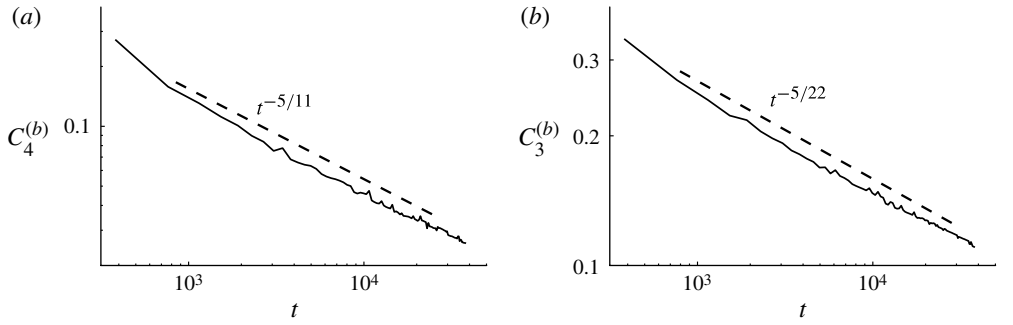

FIGURE 7. Evolution of (*a*) bound harmonics kurtosis $C_4^{(b)}$ and (*b*) skewness $C_3^{(b)}$ for swell, calculated using (2.23). Computation is limited to $k \leqslant 2.5k_p$, where k_p is the wavenumber of the spectral peak. Dashed lines show theoretical asymptotics for large time. Time is measured in characteristic wave periods, as in figure 2.

A similar computation is performed for swell and shown in figure 7. The initial condition is taken in the form of a broad energetic wavepacket, and then the evolution is computed for a long time, with the calculation of higher statistical moments. Again, the dynamic part of kurtosis is found to be negligible and the bound harmonic parts of skewness and kurtosis closely follow the theoretical asymptotes for large time. The decrease of both skewness and kurtosis slows down slightly at the end of simulations, due to the finite size of the computational domain.

5.4. *Fluctuating wind*

In nature, even when wind is nearly constant on average, it is often characterized by a considerable level of gustiness (Komen *et al.* 1994), and it is not *a priori* clear to what extent the above results are applicable to natural conditions.

In Annenkov & Shrira (2011), the field evolution of a random wave field generated by a non-stationary wind with constant mean and constant direction was studied by DNS. The main conclusion was that self-similarity of spectra evolution survives under rapidly changing forcing, and the wave spectra averaged over the forcing time scale

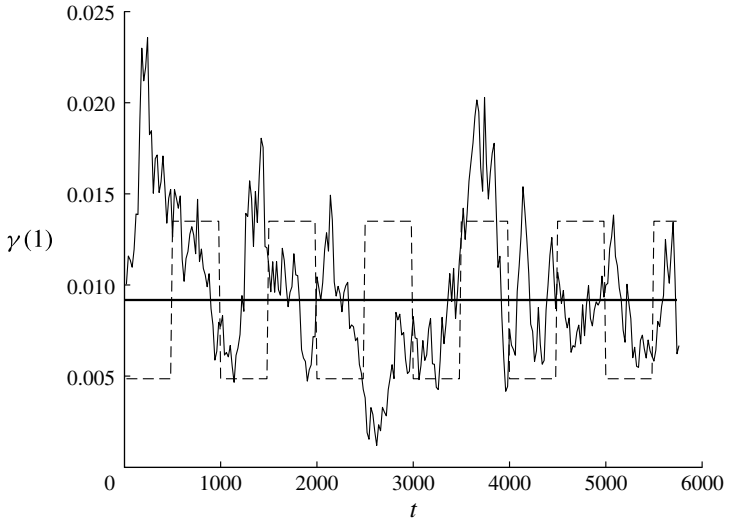

FIGURE 8. Dependence of forcing (growth rate $\gamma(\boldsymbol{k})$ at $|\boldsymbol{k}| = 1$) on time for two different models of gustiness: flip–flop wind with period equal to 1000 characteristic wave periods (dashed curve) and generic gusty wind (solid curve). The thick solid line shows constant forcing.

evolve as if the wave field was generated by a certain constant 'effective' wind. Here, we consider the evolution of skewness and kurtosis for similar fluctuating forcing. This issue has never been considered previously and the question of whether the self-similarity of higher moments survives is completely open.

For wind gustiness, we use two different models. First, we use the 'flip–flop' model, where wind speed is periodically alternating between two fixed values, 10 and 16 m s^{-1}, the period of wind oscillation T_U being in the range $40\tau \leqslant T_U \leqslant 1000\tau$, where τ is the characteristic wave period. Second, we apply a more realistic model of wind gustiness proposed by Abdalla & Cavaleri (2002), applying it to the growth rate $\gamma(\boldsymbol{k})$ instead of wind speed, to make sure that the average forcing remains the same as in the cases of constant and 'flip–flop' wind. We build a random sequence in the form

$$\xi_i = \bar{\alpha}\xi_{i-1} + \bar{\mu}_i, \tag{5.4}$$

where $\bar{\mu}_i$ is a Gaussian random number with zero mean and unity variance, $\bar{\alpha} = 0.9$ is a coherence coefficient and normalize this sequence to represent the values of $\gamma(\boldsymbol{k})$ with the mean corresponding to the average $\gamma(\boldsymbol{k})$ in the other models and the coefficient of variation (relative standard deviation) 0.2. Dependence of forcing on time for both gustiness models is shown in figure 8. Figure 9 shows a sample of evolution of the dynamic kurtosis $C_4^{(d)}$ for the case of realistic gusty wind. In figure 10, evolution of bound harmonics skewness and kurtosis is shown for the constant, periodically changing and gusty wind.

Thus, we can conclude that the assumed smallness and rapid decay of $C_4^{(d)}$ and predicted self-similar behaviour of moments proved to be very robust. Both hold even in the situations of gusty wind where, strictly speaking, no theoretical foundation for such a behaviour has been developed yet.

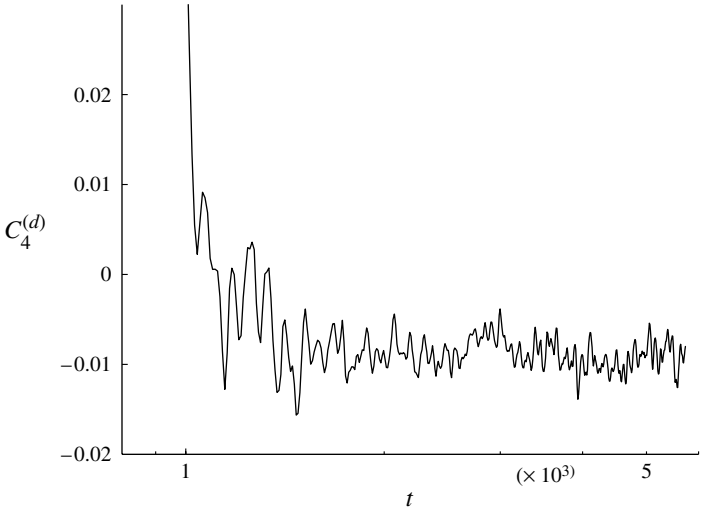

FIGURE 9. Evolution of dynamic kurtosis $C_4^{(d)}$ for a wave field generated by gusty wind according to (5.4) with the mean equal to constant wind 13.5 m s^{-1} and variance 0.2. The dynamic kurtosis is calculated using (2.8)–(2.9). Integration in (2.8) is performed over the resonant and approximately resonant nonlinear interactions taken into account in the DNS of the spectral evolution, with averaging over 30 realizations. The part of the spectrum under the direct wind forcing ($\omega > 3.13$ s^{-1}) is excluded from the computations. Time is measured in characteristic wave periods, as in figure 2.

6. Discussion

In nature wind–wave fields developing under a constant or fluctuating winds are invariably broadband, except for a relatively short initial stage (Young 1999). Evolution of spectra of such broadband fields is well-described within the conceptual framework of weak turbulence (Komen *et al.* 1994; Pushkarev *et al.* 2003). In this work we are concerned with the evolution of higher moments of surface elevation of broadband wave fields within the same weak turbulence framework. Thus, the narrowband wave fields, which attracted most of the attention in the context of abnormal wave statistics, are not considered. Strictly speaking, these narrowband situations, characterized by the Benjamin–Feir index (BFI) criterion BFI > 1 (Janssen 2003), are outside the realm of the classical weak turbulence paradigm. In this paradigm (e.g. Zakharov *et al.* 1992), random weakly nonlinear waves interact via nonlinear resonant interactions. Here we confine our attention to the lowest-order resonant interactions for gravity water waves, i.e. the quartet interactions.

The essential feature of this work is the clear separation of the two different contributions to non-Gaussianity of a wave field: dynamic non-Gaussianity, linked to nonlinear resonant interactions, and bound harmonic non-Gaussianity, present in any wave field with finite amplitude and eliminated by the canonical transformation. This separation is possible only if the dynamic non-Gaussianity is small (the dynamic kurtosis $C_4^{(d)} \ll 1$). Strictly speaking, this smallness is also the necessary condition for the weak turbulence paradigm to hold. However, this crucial condition has never been verified *a posteriori* within weak turbulence models, and little is known about the evolution of the dynamic non-Gaussianity of a generic broadband wave field, apart

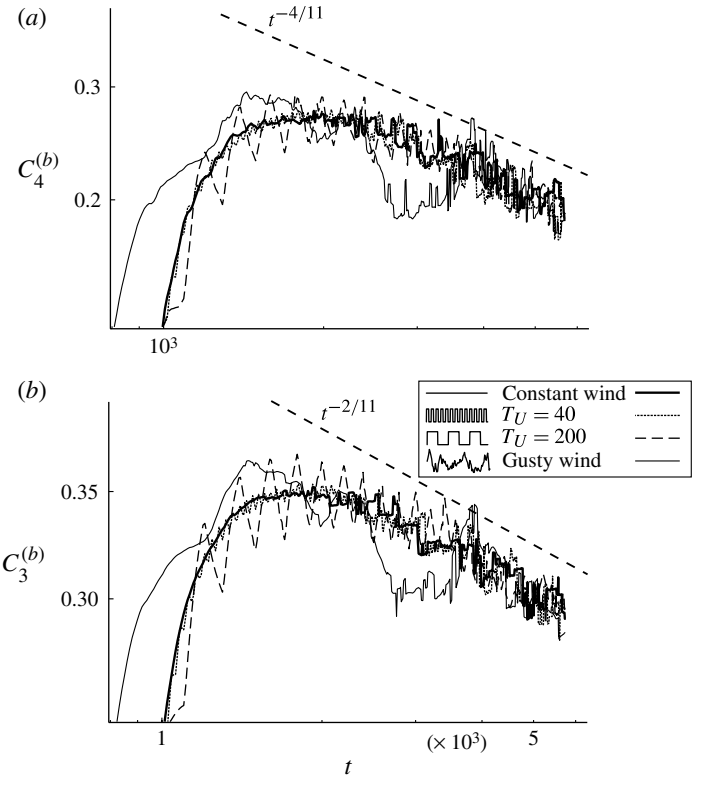

FIGURE 10. Evolution of (*a*) bound harmonic kurtosis and (*b*) skewness. Waves are generated by wind changing instantly with period T_U equal to 40 or 200 characteristic wave periods, by constant wind 13.5 m s^{-1}, corresponding to the average of linear growth rate, and by gusty wind forcing with the same mean and relative standard deviation 0.2. Computation is limited to $k \leqslant 2.5k_p$, where k_p is the wavenumber of the spectral peak. The initial part of the evolution is not shown. Dashed lines show theoretical asymptotics for large time, for the constant forcing case. Time is measured in characteristic wave periods, as in figure 2.

from the numerical observation made earlier by Annenkov & Shrira (2009*b*) that the dynamic kurtosis $C_4^{(d)}$ is negligibly small.

In this paper this observation has been extended to a wider range of situations and supported in three independent ways. First, it was verified by the DNS for generic situations of waves developing under a constant or fluctuating wind for a wide range of winds. It was found that $C_4^{(d)}$ is small (of the order $O(10^{-2})$), negative and approximately scales with the constant wind speed U as U^2. Second, for the first time $C_4^{(d)}$ was found by evaluating directly the six-dimensional integral derived by Janssen (2003). The numerical method developed for evaluating this integral for an arbitrary spectrum with the account for all (resonant and non-resonant) interactions can be used for finding the dynamic kurtosis for a wide class of situations where its value might be important. We have used the method to demonstrate the smallness of $C_4^{(d)}$ for the spectra obtained by the DNS. The U^2 scaling with wind was confirmed. The method also provided us with an insight into what interactions contribute to the dynamic kurtosis and with what effect, the most non-trivial observation being the significant role played by the non-resonant interactions. Third, using the same numerical method

with a refined grid, we have calculated the dynamic kurtosis for the model empirical (JONSWAP) spectra corresponding to mature sea conditions, and again found it to be of the order of $O(10^{-2})$.

The specific cause of the revealed smallness of the dynamic kurtosis is not yet clear and requires a dedicated study. At this stage we can only note that according to our simulations, which will be reported elsewhere, the smallness is a feature of all broadband spectra, both close to the solutions of the KE (simulated or empirical) and artificially constructed, with no resemblance to the solutions of the KE.

The simulations carried out here for realistic spectra allowed as to conclude that the dynamic kurtosis of a wave field developing under steady wind is small (of the order of $O(10^{-2})$) for the times exceeding, by a factor two or three, the characteristic time of the onset of the nonlinear regime. Thus, the dynamic non-Gaussianity is negligible, and one can find the skewness and the kurtosis due to bound harmonics using the integral formulae by Janssen (2009). The obtained values are much larger than the dynamic kurtosis, typically in the range 0.1–0.5, and found to be slowly decreasing with time. We have derived the rate of this decrease from the known asymptotic self-similar regimes of wave spectra evolution. These regimes are characterized by powerlike dependence of various characteristics of the spectra on time, determined by the degree of homogeneity of the interaction coefficients. In this sense, these power laws are as fundamental as the exponents of spectra corresponding to the direct and inverse cascade. In this work, we have complemented these known power laws with the laws for higher statistical moments. For all self-similar regimes the kurtosis decays twice as fast as the skewness. The exponents for a few distinguished asymptotic regimes are summarized in table 1. It might be possible to deduce these exponents using just the dimensional analysis, as it was done for derivation of the spectra exponents in the pioneering work by Connaughton, Nazarenko & Newell (2003), but this line has not been pursued yet. The numerically found smallness of the dynamic kurtosis means that the bound harmonic kurtosis dominates, and that the total non-Gaussianity of a wave field can be approximately determined by calculating the bound harmonics non-Gaussianity from instantaneous wave spectra employing integral expressions derived by Janssen (2009). Thus, the already existing machinery of wave spectra forecasting can be easily extended to provide the forecasting of the skewness and the kurtosis. DNS experiments with a fluctuating (periodic or gusty) wind have shown that the properties of the higher moments and the exponents of the power law decay are remarkably robust. The dynamic non-Gaussianity remains negligible for non-steady wind, and the power decay laws hold, in an averaged sense. More precisely, the moments averaged over wind fluctuations behave as if there was an effective constant wind. Recently, the effective wind for the evolution of wave spectra under gusty forcing was discussed by Annenkov & Shrira (2011). The relation between this effective wind and the effective wind for higher moments remains an open question requiring a dedicated study.

The results of this work can be extended to other situations, in particular to wave fields where bound harmonics are more pronounced and, correspondingly, the departure of the moments from Gaussianity can be noticeably stronger. Good examples are short gravity waves near the gravity–capillary range (e.g. Longuet-Higgins 1995; Fedorov & Melville 1998) and waves in fluid of finite (but not small) depth. In the latter case the bound harmonics are the strongest for $k_0 h \sim 1$, where k_0 is the dominant wavenumber and h is the depth of the fluid. For smaller depths the triad quasi-resonances become important and the approach ceases to be applicable.

On finding the evolution of skewness and kurtosis, one can in principle express all higher moments in terms of the second, third and fourth moments, and construct a p.d.f. This goes beyond the scope of the present work. Here, one needs to be careful considering the higher moments that might be affected by breaking, not taken into account in the weakly nonlinear description.

The present study was confined to the evolution of the skewness and the kurtosis of surface elevation. In some applications, primarily in the context of remote sensing, different statistical characteristics of a wave field may be of greater interest, such as higher moments of velocities, slope distribution, asymmetry, structure functions, etc. It seems possible to extend our approach to finding the moments of these quantities, which are determined by the dominant waves. This extension is not straightforward and requires a substantial extra work.

We make no attempt to compare our results with observations. The most tempting would be to test the theory against high-quality tank data obtained in carefully controlled environment. However, we are not aware of a suitable data set of field observations. The available studies of higher moments of short gravity wind waves (Leykin *et al.* 1995; Caulliez & Guerin 2012; Zavadsky, Liberzon & Shemer 2013) are concerned with the very early stage of wave spectra evolution, which we did not consider. It should be also mentioned that the tank observations describe wave field development in terms of spatial, rather than temporal, evolution, which makes a comparison less straightforward. The theory should be reformulated accordingly, which is possible, but has not been done yet. Hence, a meaningful comparison of the presented theory and observations requires a dedicated study.

Thus, the present work gives a new conceptual picture of wave field non-Gaussianity, provides specific formulae for the evolution of skewness and kurtosis of deep water wind waves of gravity range, and also opens a number of new directions of research that seem to be promising.

Acknowledgements

The work was supported by UK NERC grant NE/I01229X/1. Computations were performed on the ClusterVision computer cluster at Keele university, and on the ECMWF supercomputing facility, the access to which is gratefully acknowledged.

Appendix. Coefficients for statistical moments

Janssen (2009) derived the following expression for the second statistical moment:

$$\langle \zeta^2 \rangle = \int E_1 \, \mathrm{d}\boldsymbol{k}_1 + \int \left(\mathscr{A}_{1,2}^2 + \mathscr{B}_{1,2}^2 + 2\mathscr{C}_{1,1,2,2} \right) E_1 E_2 \, \mathrm{d}\boldsymbol{k}_{12}, \tag{A 1}$$

where

$$\mathscr{A}_{1,2} = \frac{f_{1+2}}{f_1 f_2} \left(A^{(1)}_{1+2,1,2} + A^{(3)}_{-1-2,1,2} \right), \quad \mathscr{B}_{1,2} = \frac{1}{2} \frac{f_{1-2}}{f_1 f_2} \left(A^{(2)}_{2-1,1,2} + A^{(2)}_{1-2,2,1} \right), \tag{A 2}$$

$$\mathscr{C}_{0,1,2,3} = \frac{f_0}{f_1 f_2 f_3} \left(B^{(2)}_{0,3,2,1} + B^{(3)}_{-0,1,2,3} \right). \tag{A 3}$$

Here

$$f_1 = \left(\frac{\omega_1}{2g} \right)^{1/2}. \tag{A 4}$$

Using the expressions for the functions A and B listed in Krasitskii (1994), it is easy to show that

$$\mathscr{A}_{1,2} = g\frac{-\omega_{1+2}^2 K_{1,2} + (\omega_1+\omega_2)\left[\omega_1 K_{-2,1+2} + \omega_2 K_{-1,1+2}\right]}{4\pi\omega_1\omega_2\left[\omega_{1+2}^2 - (\omega_1+\omega_2)^2\right]}, \tag{A 5}$$

$$\mathscr{B}_{1,2} = g\frac{\omega_{1-2}^2 K_{-1,2} - (\omega_1-\omega_2)\left[\omega_1 K_{2,1-2} - \omega_2 K_{-1,1-2}\right]}{4\pi\omega_1\omega_2\left[\omega_{1-2}^2 - (\omega_1-\omega_2)^2\right]}, \tag{A 6}$$

where we have denoted

$$K_{1,2} = \boldsymbol{k}_1\boldsymbol{k}_2 + q_1q_2, \quad K_{-1,2} = -\boldsymbol{k}_1\boldsymbol{k}_2 + q_1q_2, \tag{A 7}$$

and $q = |\boldsymbol{k}|$. Expression for $\mathscr{C}_{1,1,2,2}$ is longer and can be presented in the form

$$\begin{aligned}
\mathscr{C}_{1,1,2,2} = -\frac{g^2}{32\pi^2\omega_1^2\omega_2^2}\Bigg\{ & \frac{1}{(\omega_{1+2}-\omega_1-\omega_2)^2(\omega_{1+2}+\omega_1+\omega_2)^2} \\
& \times[(\omega_1^2-\omega_2^2+\omega_{1+2}^2)(\omega_{1+2}^2K_{1,2}^2+\omega_2^2K_{-1,1+2}^2) \\
& +\omega_1^2(3\omega_1^2+\omega_2^2-\omega_{1+2}^2+4\omega_1\omega_2)K_{-2,1+2}^2 \\
& +2\omega_2(\omega_1^2\omega_2+(\omega_2+2\omega_1)(\omega_2^2-\omega_{1+2}^2))K_{1,2}K_{-1,1+2} \\
& -2\omega_1^2(\omega_{1+2}^2+(\omega_1+\omega_2)^2)K_{1,2}K_{-2,1+2}+4\omega_1^2\omega_2(\omega_1+\omega_2)K_{-1,1+2}K_{-2,1+2}] \\
& +\frac{1}{(\omega_{1-2}+\omega_1-\omega_2)^2(\omega_{1-2}-\omega_1+\omega_2)^2} \\
& \times[(\omega_1^2-\omega_2^2+\omega_{1-2}^2)(\omega_{1-2}^2K_{-1,2}^2+\omega_2^2K_{-1,1-2}^2) \\
& +\omega_1^2(3\omega_1^2+\omega_2^2-\omega_{1-2}^2-4\omega_1\omega_2)K_{2,1-2}^2 \\
& +2\omega_2(\omega_1^2\omega_2+(\omega_2+2\omega_1)(\omega_2^2-\omega_{1-2}^2))K_{1,2}K_{-1,1-2} \\
& -2\omega_1^2(\omega_{1-2}^2+(\omega_1-\omega_2)^2)K_{-1,2}K_{2,1-2}+4\omega_1^2\omega_2(\omega_2-\omega_1)K_{-1,1-2}K_{2,1-2}] \\
& +\omega_1^2\omega_2^2\left(2\omega_1^4-2\omega_2^4-(\omega_1^2-\omega_2^2)(\omega_{1-2}^2+\omega_{1+2}^2)\right)\Bigg\}.
\end{aligned} \tag{A 8}$$

Then the coefficient in brackets in (A 1),

$$\mathscr{J}_{1,2}^{(2)} = \mathscr{C}_{1,1,2,2} + \tfrac{1}{2}\mathscr{A}_{1,2}^2 + \tfrac{1}{2}\mathscr{B}_{1,2}^2, \tag{A 9}$$

can be shown to take the form

$$\begin{aligned}
\mathscr{J}_{1,2}^{(2)} = -\frac{g^2}{32\pi^2\omega_1^2\omega_2^2}\Bigg\{ & \frac{1}{(\omega_{1+2}-\omega_1-\omega_2)^2(\omega_{1+2}+\omega_1+\omega_2)^2} \\
& \times[(\omega_1^2-\omega_2^2)\omega_{1+2}^2K_{1,2}^2+\omega_2^2(\omega_{1+2}^2-2\omega_2^2-2\omega_1\omega_2)K_{-1,1+2}^2 \\
& -\omega_1^2(\omega_{1+2}^2-2\omega_1^2-2\omega_1\omega_2)K_{-2,1+2}^2+2(\omega_1^2-\omega_2^2)\omega_1\omega_2K_{-1,1+2}K_{-2,1+2} \\
& +2(\omega_2^2(\omega_1+\omega_2)^2-\omega_{1+2}^2\omega_1\omega_2)K_{1,2}K_{-1,1+2} \\
& -2(\omega_1^2(\omega_1+\omega_2)^2-\omega_{1+2}^2\omega_1\omega_2)K_{1,2}K_{-2,1+2}] \\
& +\frac{1}{(\omega_{1-2}+\omega_1-\omega_2)^2(\omega_{1-2}-\omega_1+\omega_2)^2}[(\omega_1^2-\omega_2^2)\omega_{1-2}^2K_{-1,2}^2 \\
& +\omega_2^2(\omega_{1-2}^2-2\omega_2^2+2\omega_1\omega_2)K_{-1,1-2}-\omega_1^2(\omega_{1-2}^2-2\omega_1^2+2\omega_1\omega_2)K_{2,1-2} \\
& +2(\omega_2^2(\omega_1-\omega_2)^2+\omega_{1-2}^2\omega_1\omega_2)K_{-1,2}K_{-1,1-2}
\end{aligned}$$

$$
\begin{aligned}
&- 2(\omega_1^2(\omega_1-\omega_2)^2+\omega_{1-2}^2\omega_1\omega_2)K_{-1,2}K_{2,1-2}\\
&- 2(\omega_1^2-\omega_2^2)\omega_1\omega_2K_{-1,1-2}K_{2,1-2}]\\
&+ \omega_1^2\omega_2^2(2\omega_1^4-2\omega_2^4-(\omega_1^2-\omega_2^2)(\omega_{1-2}^2+\omega_{1+2}^2))\Big\}. \qquad \text{(A 10)}
\end{aligned}
$$

In this form, it becomes evident that $\mathscr{J}_{1,2}^{(2)}$ is antisymmetric (a non-trivial fact, since $\mathscr{A}_{1,2}$ and $\mathscr{B}_{1,2}$ are both symmetric). This completes the proof that the contribution of $\mathscr{J}_{1,2}^{(2)}$ to the integral (A 1) cancels out in the general two-dimensional case.

The fourth moment has the form (Janssen 2009)

$$
\langle\zeta^4\rangle = 3\int E_1E_2\,\mathrm{d}\boldsymbol{k}_{12} + 12\int \mathscr{J}_{123}^{(4)}E_1E_2E_3\,\mathrm{d}\boldsymbol{k}_{123}, \qquad \text{(A 11)}
$$

where

$$
\mathscr{J}_{123}^{(4)} = \mathscr{A}_{1,3}\mathscr{A}_{2,3}+\mathscr{B}_{1,3}\mathscr{B}_{2,3}+2\mathscr{A}_{1,3}\mathscr{B}_{2,3}+\tfrac{1}{2}\mathscr{C}_{1+2-3,1,2,3}+\tfrac{1}{2}\mathscr{D}_{1+2+3,1,2,3}. \qquad \text{(A 12)}
$$

Coefficients $\mathscr{C}$ and $\mathscr{D}$ can be written as

$$
\begin{aligned}
\mathscr{C}_{1+2-3,1,2,3} = {}& \frac{g^2}{32\pi^2\omega_1\omega_2\omega_3}\Bigg\{-\frac{1}{(\omega_{1-3}^2-(\omega_{1+2-3}-\omega_2)^2)(\omega_{1-3}^2-(\omega_1-\omega_3)^2)}\\
&\times[[K_{-1,3}(-\omega_{1+2-3}K_{2,1-3}+\omega_2K_{-1-2+3,1-3})\\
&- K_{-1-2+3,2}(\omega_1K_{3,1-3}-\omega_3K_{-1,1-3})][\omega_{1-3}^2+(\omega_1-\omega_3)(\omega_{1+2-3}-\omega_2)]\\
&+(\omega_{1+2-3}-\omega_2+\omega_1-\omega_3)[\omega_{1-3}^2K_{-1,3}K_{-1-2+3,2}\\
&+(\omega_1K_{3,1-3}-\omega_3K_{-1,1-3})(\omega_{1+2-3}K_{2,1-3}-\omega_2K_{-1-2+3,1-3})]]\\
&-\frac{1}{(\omega_{2-3}^2-(\omega_{1+2-3}-\omega_1)^2)(\omega_{2-3}^2-(\omega_2-\omega_3)^2)}\\
&\times[[K_{-2,3}(-\omega_{1+2-3}K_{1,2-3}+\omega_1K_{-1-2+3,2-3})\\
&- K_{-1-2+3,1}(\omega_2K_{3,2-3}-\omega_3K_{-2,2-3})][\omega_{2-3}^2+(\omega_2-\omega_3)(\omega_{1+2-3}-\omega_1)]\\
&+(\omega_{1+2-3}-\omega_1+\omega_2-\omega_3)[\omega_{2-3}^2K_{-2,3}K_{-1-2+3,1}\\
&+(\omega_2K_{3,2-3}-\omega_3K_{-2,2-3})(\omega_{1+2-3}K_{1,2-3}-\omega_1K_{-1-2+3,2-3})]]\\
&+\frac{1}{(\omega_{1+2}^2-(\omega_{1+2-3}+\omega_3)^2)(\omega_{1+2}^2-(\omega_1+\omega_2)^2)}\\
&\times[[K_{1,2}(\omega_{1+2-3}K_{-3,1+2}+\omega_3K_{-1-2+3,1-2})\\
&+K_{1+2-3,3}(\omega_1K_{-2,1+2}+\omega_2K_{-1,1+2})][\omega_{1+2}^2+(\omega_1+\omega_2)(\omega_3+\omega_{1+2-3})]\\
&-(\omega_{1+2-3}+\omega_3+\omega_1+\omega_2)[\omega_{1+2}^2K_{1,2}K_{1+2-3,3}\\
&+(\omega_1K_{-2,1+2}+\omega_2K_{-1,1+2})(\omega_{1+2-3}K_{-3,1+2}+\omega_3K_{-1-2+3,1+2})]]\\
&-\frac{2}{\omega_{1+2-3}+\omega_1+\omega_2-\omega_3}\Bigg\{\frac{1}{\omega_{1+2}^2-(\omega_1+\omega_2)^2}[K_{1+2-3,3}[\omega_{1+2}^2K_{1,2}\\
&-(\omega_1K_{-2,1+2}+\omega_2K_{-1,1+2})(\omega_1+\omega_2)]\\
&+(\omega_{1+2-3}K_{-3,1+2}-\omega_3K_{-1-2+3,1+2})\\
&\times[(\omega_1+\omega_2)K_{1,2}-\omega_1K_{-2,1+2}-\omega_2K_{-1,1+2}]]+\frac{1}{\omega_{2-3}^2-(\omega_2-\omega_3)^2}\\
&\times[K_{-1-2+3,1}[\omega_{2-3}^2K_{-2,3}-(\omega_2K_{3,2-3}-\omega_3K_{-2,2-3})(\omega_2-\omega_3)]\\
&+(\omega_{1+2-3}K_{1,2-3}+\omega_1K_{-1-2+3,2-3})[(\omega_2-\omega_3)K_{-2,3}-\omega_2K_{3,2-3}
\end{aligned}
$$

$$+\omega_3 K_{-2,2-3}]] + \frac{1}{\omega_{1-3}^2 - (\omega_1-\omega_3)^2}$$
$$\times [K_{-1-2+3,2}[\omega_{1-3}^2 K_{-1,3} - (\omega_1 K_{3,1-3} - \omega_3 K_{-1,1-3})(\omega_1-\omega_3)]$$
$$+(\omega_{1+2-3}K_{2,1-3} + \omega_2 K_{-1-2+3,1-3})[(\omega_1-\omega_3)K_{-1,3}$$
$$-\omega_1 K_{3,1-3} + \omega_3 K_{-1,1-3}]] + \omega_{1+2-3}\omega_1\omega_2\omega_3$$
$$\times [-\omega_2\omega_3(\omega_3^2+\omega_2^2-\omega_{1-3}^2-\omega_{1+2}^2)$$
$$-\omega_1\omega_3(\omega_3^2+\omega_1^2-\omega_{2-3}^2-\omega_{1+2}^2)$$
$$+\omega_1\omega_2(\omega_2^2+\omega_1^2-\omega_{2-3}^2-\omega_{1-3}^2) - \omega_{1+2-3}\omega_3(\omega_3^2+\omega_{1+2-3}^2-\omega_{2-3}^2-\omega_{1-3}^2)$$
$$+\omega_{1+2-3}\omega_2(\omega_2^2+\omega_{1+2-3}^2-\omega_{2-3}^2-\omega_{1+2}^2)$$
$$+\ \omega_{1+2-3}\omega_1(\omega_{1+2-3}^2+\omega_1^2-\omega_{1-3}^2-\omega_{1+2}^2)]\Big\}\Big\} \tag{A 13}$$

$$\mathscr{D}_{1+2+3,1,2,3} = -\frac{g^2}{24\pi^2\omega_1\omega_2\omega_3(\omega_{1+2+3}^2-(\omega_1+\omega_2+\omega_3)^2)}$$
$$\times \Big\{\frac{1}{\omega_{2+3}^2-(\omega_2+\omega_3)^2}[(\omega_1+\omega_2+\omega_3)K_{-1,1+2+3}[\omega_{2+3}^2K_{2,3}-(\omega_2+\omega_3)$$
$$\times(\omega_2K_{-3,2+3}+\omega_3K_{-2,2+3})] - [(\omega_2+\omega_3)K_{2,3}-\omega_2K_{-3,2+3}-\omega_3K_{-2,2+3}]$$
$$\times[\omega_{1+2+3}^2K_{1,2+3}-\omega_1(\omega_1+\omega_2+\omega_3)K_{-1-2-3,2+3}]] + \frac{1}{\omega_{1+3}^2-(\omega_1+\omega_3)^2}$$
$$\times[(\omega_1+\omega_2+\omega_3)K_{-2,1+2+3}[\omega_{1+3}^2K_{1,3}-(\omega_1+\omega_3)$$
$$\times(\omega_1K_{-3,1+3}+\omega_3K_{-1,1+3})] - [(\omega_1+\omega_3)K_{1,3}-\omega_1K_{-3,1+3}-\omega_3K_{-1,1+3}]$$
$$\times[\omega_{1+2+3}^2K_{2,1+3}-\omega_2(\omega_1+\omega_2+\omega_3)K_{-1-2-3,1+3}]] + \frac{1}{\omega_{1+2}^2-(\omega_1+\omega_2)^2}$$
$$\times[(\omega_1+\omega_2+\omega_3)K_{-3,1+2+3}[\omega_{1+2}^2K_{1,2}-(\omega_1+\omega_2)$$
$$\times(\omega_1K_{-2,1+2}+\omega_2K_{-1,1+2})] - [(\omega_1+\omega_2)K_{1,2}-\omega_1K_{-2,1+2}-\omega_2K_{-1,1+2}]$$
$$\times[\omega_{1+2+3}^2K_{3,1+2}-\omega_3(\omega_1+\omega_2+\omega_3)K_{-1-2-3,1+2}]] + \omega_{1+2+3}^2\omega_1\omega_2\omega_3$$
$$\times[[\omega_1\omega_2(\omega_1^2+\omega_2^2-\omega_{2+3}^2-\omega_{1+3}^2)+\omega_1\omega_3$$
$$\times(\omega_1^2+\omega_3^2-\omega_{2+3}^2-\omega_{1+2}^2)+\omega_2\omega_3(\omega_2^2+\omega_3^2-\omega_{1+3}^2-\omega_{1+2}^2)]$$
$$-(\omega_1+\omega_2+\omega_3)[\omega_1(\omega_{1+2+3}^2+\omega_1^2-\omega_{1+3}^2-\omega_{1+2}^2)$$
$$+\omega_2(\omega_{1+2+3}^2+\omega_2^2-\omega_{2+3}^2-\omega_{1+2}^2)+\omega_3(\omega_{1+2+3}^2+\omega_3^2-\omega_{2+3}^2-\omega_{1+3}^2)]]\Big\}. \tag{A 14}$$

For a single wavetrain with $\boldsymbol{k} = k_0$,

$$\mathscr{A}_{00} = \frac{k_0}{2\pi}, \quad \mathscr{B}_{00} = 0, \quad \mathscr{C}_{0+0-0,0,0,0} = -\frac{k_0^2}{8\pi^2}, \quad \mathscr{D}_{0+0+0,0,0,0} = \frac{3k_0^2}{8\pi^2}. \tag{A 15}$$

It is easy to see that $\mathscr{J}_{123}^{(4)}$ is a homogeneous function of degree two:

$$\mathscr{J}^{(4)}(\alpha\boldsymbol{k}_1, \alpha\boldsymbol{k}_2, \alpha\boldsymbol{k}_3) = \alpha^2\,\mathscr{J}^{(4)}(\boldsymbol{k}_1, \boldsymbol{k}_2, \boldsymbol{k}_3). \tag{A 16}$$

REFERENCES

ABDALLA, S. & CAVALERI, L. 2002 Effect of wind variability and variable air density on wave modeling. *J. Geophys. Res.* **107** (C7), 17.

ANNENKOV, S. Y. & SHRIRA, V. I. 2001 On the predictability of evolution of surface gravity and gravity-capillary waves. *Physica* D **152–153**, 665–675.

ANNENKOV, S. Y. & SHRIRA, V. I. 2006*a* Role of non-resonant interactions in the evolution of nonlinear random water wave fields. *J. Fluid Mech.* **561**, 181–207.

ANNENKOV, S. Y. & SHRIRA, V. I. 2006*b* Direct numerical simulation of downshift and inverse cascade for water wave turbulence. *Phys. Rev. Lett.* **96**, 204501.

ANNENKOV, S. Y. & SHRIRA, V. I. 2009*a* 'Fast' nonlinear evolution in wave turbulence. *Phys. Rev. Lett.* **102**, 024502.

ANNENKOV, S. Y. & SHRIRA, V. I. 2009*b* Evolution of kurtosis for wind waves. *Geophys. Res. Lett.* **36**, L13603.

ANNENKOV, S. Y. & SHRIRA, V. I. 2011 Evolution of wave turbulence under 'gusty' forcing. *Phys. Rev. Lett.* **107**, 114502.

BABANIN, A. V. 2011 *Breaking and Dissipation of Ocean Surface Waves*. Cambridge University Press.

BADULIN, S. I., BABANIN, A. V., RESIO, D. & ZAKHAROV, V. E. 2007 Weakly turbulent laws of wind-wave growth. *J. Fluid Mech.* **591**, 339–378.

BADULIN, S. I., PUSHKAREV, A. N., RESIO, D. & ZAKHAROV, V. E. 2005 Self-similarity of wind-driven seas. *Nonlinear Process. Geophys.* **12**, 891–946.

CAULLIEZ, G. & GUERIN, C.-A. 2012 Higher-order statistical analysis of short wind wave fields. *J. Geophys. Res.* **117**, C06002.

CONNAUGHTON, C., NAZARENKO, S. & NEWELL, A. C. 2003 Dimensional analysis and weak turbulence. *Physica* D **184**, 86–97.

DONELAN, M. A., BABANIN, A. V., YOUNG, I. R. & BANNER, M. L. 2006 Wave-follower field measurements of the wind-input spectral function. Part II. Parameterization of the wind input. *J. Phys. Oceanogr.* **36**, 1672–1679.

FEDELE, F. 2008 Rogue waves in oceanic turbulence. *Physica* D **237**, 2127–2131.

FEDELE, F. & TAYFUN, M. A. 2009 On nonlinear wave groups and crest statistics. *J. Fluid Mech.* **620**, 221–239.

FEDOROV, A. V. & MELVILLE, W. K. 1998 Nonlinear gravity-capillary waves with forcing and dissipation. *J. Fluid Mech.* **354**, 1–42.

GABOR, D. 1946 Theory of communication. *J. Inst. Elect. Eng.* **93**, 429–457.

GAGNAIRE-RENOUD, E., BENOIT, M. & BADULIN, S. I. 2011 On weakly turbulent scaling of wind sea in simulations of fetch-limited growth. *J. Fluid Mech.* **669**, 178–213.

GODA, Y. 2000 *Random Seas and Design of Maritime Structures*. World Scientific.

HASSELMANN, K. 1962 On the nonlinear energy transfer in a gravity-wave spectrum. Part 1. General theory. *J. Fluid Mech.* **12**, 481–500.

HASSELMANN, K., BARNETT, T. P., BOUWS, E., CARLSON, H., CARTWRIGHT, D.E., ENKE, K., EWING, J. A., GIENAPP, H., HASSELMANN, D. E., KRUSEMAN, P., MEERBURG, A., MÜLLER, P., OLBERS, D. J., RICHTER, K., SELL, W. & WALDEN, H. 1973 Measurements of wind wave growth and swell decay during the Joint North Sea Wave Project (JONSWAP). In *Deutsche hydrographische Zeitschrift: Ergaenzungsheft: Reihe A*, 12. Deutsches Hydrographisches Institut.

HASSELMANN, K., ROSS, D. B., MÜLLER, P. & SELL, W. 1976 A parametric wave prediction model. *J. Phys. Oceanogr.* **6**, 200–228.

HSIAO, S. V. & SHEMDIN, O. H. 1983 Measurements of wind velocity and pressure with a wave follower during MARSEN. *J. Geophys. Res.* **88**, 9841–9849.

JANSSEN, P. A. E. M. 2003 Nonlinear four-wave interactions and freak waves. *J. Phys. Oceanogr.* **33**, 863–884.

JANSSEN, P. A. E. M. 2004 *The Interaction of Ocean Waves and Wind*. Cambridge University Press.

JANSSEN, P. A. E. M. 2007 On the probability density function of wave height and wave period. ECMWF Research Department Memorandum, 22 June 2007.

JANSSEN, P. A. E. M. 2008 Progress in ocean wave forecasting. *J. Comput. Phys.* **227**, 3572–3594.

JANSSEN, P. A. E. M. 2009 On some consequences of the canonical transformation in the Hamiltonian theory of water waves. *J. Fluid Mech* **637**, 1–44.

JANSSEN, P. A. E. M. & BIDLOT, J.-R. 2009 On an extension of the freak wave warning system and its verification. In *ECMWF Technical Memorandum No. 588*. European Centre for Medium-Range Weather Forecasts, Reading, UK.

KOMEN, G. J., CAVALERI, L., DONELAN, M., HASSELMANN, K., HASSELMANN, S. & JANSSEN, P. A. E. M. 1994 *Dynamics and Modelling of Ocean Waves*. Cambridge University Press.

KRASITSKII, V. P. 1994 On reduced Hamiltonian equations in the nonlinear theory of water surface waves. *J. Fluid Mech.* **272**, 1–20.

KUDRYAVTSEV, V. N., MAKIN, V. K. & MEIRINK, J. F. 2001 Simplified model of the airflow above waves. *Bound.-Layer Meteor.* **100**, 63–90.

LONGUET-HIGGINS, M. S. 1957 The statistical analysis of a random, moving surface. *Phil. Trans. R. Soc. Lond.* **A 249**, 321–387.

LONGUET-HIGGINS, M. S. 1983 On the joint distribution of wave periods and amplitudes in a random wave field. *Proc. R. Soc. Lond.* **A 389**, 241–258.

LONGUET-HIGGINS, M. S. 1995 Parasitic capillary waves: a direct calculation. *J. Fluid Mech.* **301**, 79–107.

LEYKIN, I. A., DONELAN, M. A., MELLEN, R. H. & MCLAUGHLIN, D. J. 1995 Asymmetry of wind waves studied in a laboratory tank. *Nonlinear Process. Geophys.* **2**, 280–289.

LVOV, Y. V., NAZARENKO, S. & POKORNI, B. 2006 Discreteness and its effect on water-wave turbulence. *Physica* D **218**, 24–35.

MORI, N. & JANSSEN, P. A. E. M. 2006*a* Freak wave prediction from directional spectra. In *Coastal Engineering 2006, Proceedings of the 30th International Conference* (ed. J. M. Smith), pp. 714–725. World Scientific.

MORI, N. & JANSSEN, P. A. E. M. 2006*b* On kurtosis and occurrence probability of freak waves. *J. Phys. Oceanogr.* **36**, 1471–1483.

NAZARENKO, S. V. 2011 *Wave Turbulence*. Springer.

ONORATO, M., OSBORNE, A. R., SERIO, M., CAVALERI, L., BRANDINI, C. & STANSBERG, C. T. 2006 Extreme waves, modulational instability and second-order theory: wave flume experiments on irregular waves. *Eur. J. Mech. (*B/*Fluids*) **25**, 586–601.

PUSHKAREV, A., RESIO, D. & ZAKHAROV, V. E. 2003 Weak turbulent approach to the wind-generated gravity sea waves. *Physica* D **184**, 29–63.

PUSHKAREV, A. N. & ZAKHAROV, V. E. 2000 Turbulence of capillary waves – theory and numerical simulation. *Physica* D **135**, 98–116.

RICE, S. O. 1954 Mathematical analysis of random noise. In *Reprinted of the 1944 original in Selected Papers on Noise and Stochastic Processes* (ed. N. Wax), pp. 133–294. Dover.

STANSELL, P. 2004 Distributions of freak wave heights measured in the North Sea. *Appl. Ocean Res.* **26**, 35–48.

TAYFUN, M. A. 1980 Narrow-band nonlinear sea waves. *J. Geophys. Res* **85**, 1548–1552.

TOBA, Y. 1972 Local balance in the air–sea boundary processes. Part I. On the growth process of wind waves. *J. Oceanogr. Soc. Japan* **28**, 109–121.

TOBA, Y. 1973 Local balance in the air–sea boundary processes. Part III. On the spectrum of wind waves. *J. Oceanogr. Soc. Japan* **29**, 209–220.

YOUNG, I. R. 1999 *Wind Generated Ocean Waves*. Elsevier.

ZAKHAROV, V. E. 1968 Stability of periodic waves of finite amplitude on the surface of a deep fluid. *J. Appl. Mech. Tech. Phys. (USSR)* **9**, 86–94.

ZAKHAROV, V. E. 2005 Theoretical interpretation of fetch limited wind-driven sea observations. *Nonlinear Proc. Geophys.* **12**, 1011–1020.

ZAKHAROV, V. E. & ZASLAVSKY, M. M. 1983 Dependence of wave parameters on the wind velocity, duration of its action and fetch in the weak-turbulence theory of water waves. *Izv. Atmos. Ocean. Phys.* **19**, 300–306.

ZAKHAROV, V. E., L'VOV, V. S. & FALKOVICH, G. 1992 *Kolmogorov Spectra of Turbulence I: Wave Turbulence*. Springer.

ZAVADSKY, A., LIBERZON, D. & SHEMER, L. 2013 Statistical analysis of the spatial evolution of the stationary wind-wave field. *J. Phys. Oceanogr.* **43**, 65–79.